Gluon radiation off hard quarks in a nuclear environment: opacity expansion

Urs Achim Wiedemann
Theory Division, CERN, CH-1211 Geneva 23, Switzerland
(February 1, 2008)

We study the relation between the Baier-Dokshitzer-Mueller-Peigné-Schiff (BDMPS) and Zakharov formalisms for medium-induced gluon radiation off hard quarks, and the radiation off very few scattering centers. Based on the non-abelian Furry approximation for the motion of hard partons in a spatially extended colour field, we derive a compact diagrammatic and explicitly colour trivial expression for the N-th order term of the $\mathbf{k}_\perp$-differential gluon radiation cross section in an expansion in the opacity of the medium. Resumming this quantity to all orders in opacity, we obtain Zakharov's path-integral expression (supplemented with a regularization prescription). This provides a new proof of the equivalence of the BDMPS and Zakharov formalisms which extends previous arguments to the $\mathbf{k}_\perp$-differential cross section. We give explicit analytical results up to third order in opacity for both the gluon radiation cross section of free incoming and of in-medium produced quarks. The N-th order term in the opacity expansion of the radiation cross section is found to be a convolution of the radiation associated to N-fold rescattering and a readjustment of the probabilities that rescattering occurs with less than N scattering centers. Both informations can be disentangled by factorizing out of the radiation cross section a term which depends only on the mean free path of the projectile. This allows to infer analytical expressions for the totally coherent and totally incoherent limits of the radiation cross section to arbitrary orders in opacity.

I. INTRODUCTION

Hard partons, produced in relativistic heavy ion collisions at RHIC and LHC, will undergo multiple rescattering inside the nuclear environment before entering the hadronization process outside the nuclear environment (or in a very dilute one). This follows from standard formation time arguments. Prior to hadronization, medium-induced radiative energy loss is expected to be the main medium modification encountered by hard partons. The size of this effect depends on the density and nature of the medium and may be significantly enhanced in a deconfined partonic medium [1, 2]. A corresponding strong medium-modification of the high-pt tails of hadronic single particle spectra ("jet quenching") [3, 4] is thus a tentative signal for the formation of a deconfined state. This possibility has motivated many studies of medium-induced gluon radiation in recent years [5, 6, 7, 8, 9, 10, 11, 12, 13, 14, 15, 16, 17, 18].

Most recent studies of the non-abelian energy loss are carried out within the Gyulassy-Wang (GW) model [1] which mimics the medium by a set of coloured static scattering centers. Despite its simplicity, this model is of phenomenological interest, since the medium-induced radiative energy loss belongs to those observables which depend mainly on the average transverse colour field strength encountered by the parton rather than on the model-specific details with which this colour field strength is described [19].

First studies of the GW model [1, 2] focussed on the rescattering of the hard quark and arrived at a radiative energy loss $dE/dx = \text{const}$ independent of the path length. Baier-Dokshitzer-Mueller-Peigné-Schiff (BDMPS) [6] established later that gluon rescattering diagrams give the dominant contribution. They found a potentially dramatic linear increase $dE/dx \propto L$ of the energy loss with the medium thickness L. This can be understood in terms of an uncertainty argument of Brodsky and Hoyer [20] which relates the average transverse gluon momentum $\langle \mathbf{k}_\perp^2 \rangle$ to the radiative energy loss $dE/dx \propto \langle \mathbf{k}_\perp^2 \rangle$. Brownian motion of the rescattering gluon then implies $\langle \mathbf{k}_\perp^2 \rangle \propto L$ and the quadratic L-dependence of radiative energy loss in the BDMPS formalism. While all these studies start from the complete set of multiple scattering diagrams, Zakharov [5, 8] has advocated a different and very elegant approach to the same problem. In his path-integral formalism, the radiation cross section is determined by a dipole cross section which essentially measures the difference between elastic scattering amplitudes of different projectile Fock state components as a function of impact parameter. Baier, Dokshitzer, Mueller and Schiff (BDMS) have shown [10] that the evolution of the rescattering amplitude in the BDMPS-formalism is determined by Zakharov's dipole cross section.

The above mentioned calculations do not have a clear connection to experiment since the total radiative energy loss dE/dx is not an experimental observable. Unlike the situation in QED where the charged projectile can in principle be arbitrarily well separated from its radiation, medium-induced QCD bremsstrahlung is only an observable to the extent to which it is emitted kinematically well separated outside the typical hadronization cone of the hard parton. Realistic energy loss estimates thus require knowledge about the $\mathbf{k}_\perp$-differential gluon radiation spectrum. First calculations of this observable were published a year ago in the Zakharov [12, 13] and in the BDMPS-formalism [14]. These studies contain essential steps towards a phenomenological application: especially,

Ref. [12] shows how to rewrite Zakharov's path-integral formalism in a simple, numerically accessible form, and Ref. [14] gives results for the radiation outside the kinematically unresolvable hadronization cone of the parton.

However, calculating the angular distribution is not the only problem in making contact with phenomenology. Another problem is that the concept of a homogeneous medium of finite extent, underlying the BDMPS and Zakharov formalisms, may not be applicable to heavy ion collisions at RHIC and LHC. Unlike the situation in QED, where even the thinnest targets probed in experiments of the Landau-Pomeranchuk- Migdal effect amount to $\approx 10000 - 100000$ small-angle scatterings, one expects for the medium-induced radiation off hard partons in relativistic heavy ion collisions a much smaller average number of rescatterings, say $\approx 2 - 10$ [17]. A comparison of the BDMPS- and Zakharov- formalisms with results for a small fixed number $N = 1, 2, 3, \ldots$ of rescatterings is needed to understand to what extent the concept of a homogeneous medium can be justified for such an extremely thin medium. The only existing studies [12, 17] of scenarios with very few $N \leq 3$ scattering centers assume implicitly an exclusive measurement of jet, gluon and recoil target partons. They are thus restricted to the study of a subclass of all available rescattering diagrams, and their results do not compare directly to the BDMPS and Zakharov formalisms (see below for more details). It is one of the results of the present paper to calculate the gluon radiation spectrum for a "medium" of very few $N \leq 3$ scattering centers, including all available rescattering diagrams, thus allowing for a direct comparison. More generally, we discuss in which sense the N-th order term in the opacity expansion of Zakharov's result is related to radiation off a target of a fixed number N of scattering centers.

From a technical point of view, the present work is an application and extension of methods developped in [19]. There, we have derived the non-abelian Furry approximation for the wavefunction of a hard parton which undergoes multiple rescattering in a spatially extended colour field. This Furry wavefunction provides a compact shorthand for the high-energy limit of the complete class of final state rescattering diagrams. Relevant for the present work is that we have developped in Ref. [19] diagrammatic tools to determine under which conditions observables of a multiple partonic rescattering process are colour trivial. *Colour triviality* is the remarkable fact that for some rescattering processes, the sum of all contributions to the N-fold rescattering depends on a unique N-th power of the $SU(3)$ Casimir operators, rather than to depend on colour interference terms associated to more than one colour trace. This renders the calculational problem essentially abelian and is crucial for going beyond very few rescatterings where brute force perturbative calculations are still feasible. Colour triviality is thus an important property in the study of non-abelian gluon bremsstrahlung.

The present work applies the non-abelian Furry approximation to the calculation of the medium-induced gluon radiation cross section. In section II, we derive the radiation cross section in terms of Furry wavefunctions. From this, we derive in section III a set of diagrammatic identities which automate the proof of colour triviality. In section IV, these identities are applied to derive an explicitly colour trivial diagrammatic expression for the N-th order term of the opacity expansion of the $\mathbf{k}_\perp$-differential gluon radiation spectrum. Contact with analytical expressions is made by showing that the sum over all N-th order contributions results in a path-integral expression which essentially coincides with Zakharov's result. In section V, we relate this path-integral expression to the radiation off a target of a fixed number of scattering centers. All calculations in sections II-V are for gluon radiation off an idealized free *in*coming quark which satisfies plane wave boundary conditions at far backward position. The corresponding radiation cross sections are denoted by a superscript (in). In section VI, we extend these calculations to the radiation off *nascent* quarks produced in the medium. The gluon radiation cross section associated with them is characterized by a superscript (nas) and gives access to the interference pattern between hard and medium-dependent radiation. The main results and further perspectives are finally discussed in the Conclusions.

II. THE FORMALISM

We consider gluon radiation off a hard quark which undergoes multiple elastic rescattering in a spatially extended colour field. The gluon of momentum $k = (\omega, \mathbf{k})$ carries away a fraction x of the totally available energy of the initial parton, $\omega = x\, E_1$. A typical contribution to the radiation amplitude is shown in Fig. 1. For the coloured potential describing the medium, we choose the ansatz of the Gyulassy-Wang model [1]

$$A_\mu^{(q)}(\mathbf{x})_{a\,b} = \delta_{0\mu} \sum_{i=1}^{\infty} \varphi_i^d(\mathbf{x}) \, \left(T^d\right)_{a\,b} , \tag{2.1}$$

$$A_\mu^{(g)}(\mathbf{x})_{a\,b} = \delta_{0\mu} \sum_{i=1}^{\infty} \varphi_i^d(\mathbf{x}) \, \left(i\, f^{adb}\right) , \tag{2.2}$$

$$\varphi_i^d(\mathbf{x}) = \varphi(\mathbf{x} - \check{\mathbf{x}}_i)\, \delta^{d\,d_i} . \tag{2.3}$$

The static scattering potentials $\varphi_i^d(\mathbf{x})$ show a sufficiently rapid (e.g. Yukawa-type) spatial fall-off. At the i-th scattering center, a specific colour charge $d = d_i$ is exchanged. T^d, $(d = 1, \ldots, N_c^2 - 1)$, denotes the generators of the $SU(N_c)$ fundamental representation, and the totally antisymmetric structure constants f_{abc} denote the adjoint representation. The latter appears in the rescattering amplitude of the emitted gluon.

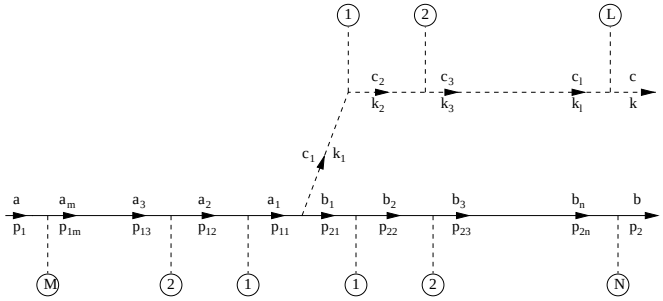

FIG. 1. Contribution to the gluon radiation amplitude (2.4), involving M-, L-, and N-fold rescattering of the in- and outgoing partons respectively.

Summed over arbitrary many rescatterings, the gluon radiation amplitude $\mathcal{M}_{a\to b\,c}$ in this extended colour potential takes the form

$$\mathcal{M}_{a\to b\,c} = \int d^3\mathbf{y}\, I_{a\,a_1}(\mathbf{y},p_1)\,\left(-i\,g_s\,\gamma_{\mu_1}\,(T^{c_1})_{a_1\,b_1}\right) \times e^{-\epsilon|y_l|}\, I^{\mu_1}_{c_1\,c}(\mathbf{y},k)\, I_{b_1\,b}(\mathbf{y},p_2)\,. \quad (2.4)$$

Here, the term $e^{-\epsilon|y_l|}$ is the adiabatic switching off of the interaction term at large distances. In our calculation, the limit $\epsilon\to 0$ does not commute with the longitudinal y_l-integral, and this regularization has to be carried through intermediate steps of the calculation [12]. To explain the notation of (2.4), we consider the typical diagrammatic contribution given in Fig. 1. The N-fold rescattering of the quark, emitted from the radiation vertex with momentum p_{21} and colour b_1, and appearing in the final state with momentum p_2 and colour b is determined by the component $I^{(N)}_{b_1\,b}$ of [see Fig. 1 for details of notation]

$$I^{(N)}(\mathbf{y},p_2) = e^{-i\,\mathbf{p}_{2,1}\cdot\mathbf{y}}\,\mathcal{P}\,\left(\prod_{i=1}^{N}\int\frac{d^3\mathbf{p}_{2,i}}{(2\pi)^3}\,d^3\mathbf{x}_i \times\frac{i\,(\not{p}_{2,i}+m)\,\gamma_0}{p_{2,i}^2-m^2+i\,\epsilon}[-i\,A_0^{(q)}(\mathbf{x}_i)] \times\; e^{-i\,\mathbf{x}_i\cdot(\mathbf{p}_{2,i+1}-\mathbf{p}_{2,i})}\right)\,v(\mathbf{p_2})\,. \quad (2.5)$$

Here, the path-ordering $\mathcal{P}$ implies that $A_0^{(q)}(\mathbf{x}_{i+1})$ stands to the right of $A_0^{(q)}(\mathbf{x}_i)$, and the momentum transfers to the quark line are written as Fourier transforms of the static scattering potential with respect to the relative momenta $\mathbf{p}_{2,i+1}-\mathbf{p}_{2,i}$. $v(\mathbf{p_2})$ is the spinor of the outgoing quark. In complete analogy, rescattering effects of the incoming quark are described by the component $I^{(M)}_{a\,a_1}$ of

$$I^{(M)}(\mathbf{y},p_1) = v^\dagger(\mathbf{p_1})\,\mathcal{P}\,\left(\prod_{i=1}^{M}\int\frac{d^3\mathbf{p}_{1,i}}{(2\pi)^3}\,d^3\mathbf{x}_i \times[-i\,A_0^{(q)}(\mathbf{x}_i)]\frac{i\,(\not{p}_{1,i}+m)\,\gamma_0}{p_{1,i}^2-m^2+i\,\epsilon} \times\; e^{-i\,\mathbf{x}_i\cdot(\mathbf{p}_{1,i+1}-\mathbf{p}_{1,i})}\right)\,e^{i\,\mathbf{p}_{1,1}\cdot\mathbf{y}}\,\gamma_0\,, \quad (2.6)$$

and the rescattering effects on the emitted gluon are taken into account by the component $I^{\mu_1\,(L)}_{c_1\,c}$ of

$$I^{\mu_1\,(L)}(\mathbf{y},k) = e^{-i\,\mathbf{k}_1\cdot\mathbf{y}}\,\mathcal{P}\,\left(\prod_{i=1}^{L}\int\frac{d^3\mathbf{k}_i}{(2\pi)^3}\,d^3\mathbf{x}_i \times[-i\,A_0^{(g)}(\mathbf{x}_i)]\frac{-i\,g^{\mu_i\,\mu_i'}}{k_i^2-m^2+i\,\epsilon}V_{\mu_i'0\mu_i} \times\; e^{-i\,\mathbf{x}_i\cdot(\mathbf{k}_{i+1}-\mathbf{k}_i)}\right)\,\epsilon^{\mu_L}\,, \quad (2.7)$$

where ϵ^{μ_L} is the polarization of the gluon. To calculate the high-energy limit of the radiation spectrum, one has to keep on the amplitude level the leading order in norm and the next-to-leading order in the phase. In this limit, other scattering contributions (e.g. those involving the 4-gluon-vertex) are negligible [6], and the expressions (2.5)-(2.7) take the form of non-abelian Furry wavefunctions [19]. In appendix A, we show that by approximating $I^{\mu_1\,(L)}(\mathbf{y},k)$ to leading order $O(1/\omega)$ in the norm and next to leading order in the phase, the corresponding sum over arbitrary many rescattering centers takes a particularly simple form

$$I^{\mu_1}(\mathbf{y},k) = \sum_{L=0}^{\infty} I^{\mu_1\,(L)}(\mathbf{y},k) = \epsilon^{\mu_1}\,e^{-i\,\mathbf{k}_1\cdot\mathbf{y}}\int d\mathbf{x}_\perp G_{(g)}(\mathbf{y};\mathbf{x}|\omega)\,F(\mathbf{x},\mathbf{k})\,. \quad (2.8)$$

Here, $F(\mathbf{x},\mathbf{k})$ denotes the asymptotic plane wave

$$F(\mathbf{x}_\perp,x_l,\mathbf{p}_2) = \exp\left\{-i\,\mathbf{p}_2^\perp\cdot\mathbf{x}_\perp + i\,\frac{\mathbf{p}_2^{\perp\,2}}{2\,p_2}x_l\right\}\,, \quad (2.9)$$

and the Green's function $G_{(g)}$ is an approximate solution of the non-abelian Dirac equation in the spatially extended colour potential $A_0^{(q)}$. This Green's function describes the leading transverse deviation of the rescattering parton from a straight line propagation. It can be represented in terms of a path-integral over a path-ordered Wilson line $W_{(g)}\big([\mathbf{r}];z,z'\big)$,

$$G_{(g)}(\mathbf{r},z;\mathbf{r}',z'|p) = = \int\mathcal{D}\boldsymbol{r}(\xi)\,\exp\left\{\frac{ip}{2}\int_z^{z'}d\xi\,\dot{\mathbf{r}}^2(\xi)\right\}\,W\big([\mathbf{r}];z,z'\big)\,, \quad (2.10)$$

$$W_{(g)}\big([\mathbf{r}];z,z'\big) = \mathcal{P}\,\exp\left\{-i\int_z^{z'}d\xi\,A_0^{(g)}(\mathbf{r}(\xi),\xi)\right\}\,. \quad (2.11)$$

In what follows, we shall explicitly denote or supress the longitudinal coordinates of these Green's functions, depending on whether this information can be easily inferred.

In analogy to (2.8), we have shown in a previous paper [19] that the sum over an arbitrary number of final state

rescatterings of the outgoing quark takes the compact form

$$I(\mathbf{y},p_2)=\sum_{N=0}^{\infty} I^{(N)}(\mathbf{y},p_2)$$
$$=e^{-i\,p_2\,y_l}\,\hat{D}_2\int d\mathbf{x}_\perp\,G_{(q)}(\mathbf{y};\mathbf{x}|p_2)F(\mathbf{x},\mathbf{p}_2)\,v(\mathbf{p}_2)\,. \quad (2.12)$$

As denoted by the subscript (q), the Green's function contains in this case a Wilson line in the fundamental quark representation of $SU(N_c)$. The only new ingredient compared to (2.8) is the differential operator $\hat{D}_i$ [11, 12]

$$\hat{D}_i=1-i\,\frac{\boldsymbol{\alpha}\cdot\boldsymbol{\nabla}}{2\,E_i}-\frac{\boldsymbol{\alpha}\cdot(\mathbf{p}_i-\mathbf{n}\,p_i)}{2\,E_i}\,,$$
$$\boldsymbol{\alpha}=\gamma_0\,\boldsymbol{\gamma}\quad;\quad z=\boldsymbol{n}\cdot\boldsymbol{x}\quad;\quad p_i=|\boldsymbol{p}_i|\,. \quad (2.13)$$

This operator contains in a configuration space formulation the $O(1/E)$ corrections to the propagator of momentum p_{21}. Inclusion of these corrections for the fermion propagators entering the radiation vertex is necessary, since the leading $1/E$-contribution cancels due to the Bloch-Nordsieck structure of the radiation vertex [19].

In terms of the Green's functions $G_{(q)}$ and $G_{(g)}$, the gluon radiation amplitude (2.4) takes the form

$$\mathcal{M}_{a\to b\,c}=-i\int dy_l\,e^{i\,\bar{q}\,y_l}\,e^{-\epsilon\,|y_l|}\int d^2\mathbf{y}$$
$$\times\int d^2\mathbf{x}_1\,d^2\mathbf{x}_2\,d^2\mathbf{x}_g\,e^{i\mathbf{x}_{1\perp}\cdot\mathbf{p}_{1\perp}-i\mathbf{x}_{2\perp}\cdot\mathbf{p}_{2\perp}-i\mathbf{x}_{g\perp}\cdot\mathbf{k}_\perp}$$
$$\times G^{aa_1}_{(q)}(\mathbf{x}_1;\mathbf{y}|p_1)\,\hat{\Gamma}_{\mathbf{y}}\,(T^{c_1})_{a_1b_1}\,G^{c_1c}_{(g)}(\mathbf{y};\mathbf{x}_g|\omega)$$
$$\times G^{b_1b}_{(q)}(\mathbf{y};\mathbf{x}_2|p_2)\,e^{-i\frac{\mathbf{p}_{1\perp}^2}{2p_1}x_l+i\frac{\mathbf{p}_{2\perp}^2}{2p_2}x_l-i\frac{\mathbf{k}_\perp^2}{2\omega}x_l}\,. \quad (2.14)$$

Here, we have used the fraction x of the incident energy carried by the emitted gluon, $\omega=x\,E_1$, to write

$$\bar{q}=p_1-p_2-\omega=\frac{x\,m_q^2}{2\,(1-x)\,E_1}\,. \quad (2.15)$$

Also, we have introduced the interaction vertex $\hat{\Gamma}$ as the notational shorthand for the spinor structure of the amplitude (2.14),

$$\hat{\Gamma}_{\mathbf{y}}=v^\dagger(p_1)\,\hat{D}_1\gamma_0\,\epsilon\cdot\gamma\,\hat{D}_2\,v(p_2)\,. \quad (2.16)$$

This leads to the radiation probability

$$\langle|\mathcal{M}_{a\to b\,c}|^2\rangle=2\,\mathrm{Re}\int_{z_-}^{z_+}dy_l\int_{y_l}^{z_+}d\bar{y}_l\,e^{i\bar{q}(y_l-\bar{y}_l)}$$
$$\times e^{-\epsilon\,|y_l|-\epsilon\,|\bar{y}_l|}\int d\mathbf{y}\,d\bar{\mathbf{y}}\,d\mathbf{x}_1\,d\bar{\mathbf{x}}_1\,d\mathbf{x}_2\,d\bar{\mathbf{x}}_2\,d\mathbf{x}_g\,d\bar{\mathbf{x}}_g\,\hat{\Gamma}_{\mathbf{y}}\,\hat{\Gamma}^\dagger_{\bar{\mathbf{y}}}$$
$$\times G^{aa_1}_{(q)}(\mathbf{x}_1;\mathbf{y}|p_1)\,T^{c_1}_{a_1b_1}\,G^{c_1c}_{(g)}(\mathbf{y};\mathbf{x}_g|\omega)\,G^{b_1b}_{(q)}(\mathbf{y};\mathbf{x}_2|p_2)$$
$$\times G^{b\bar{b}_1}_{(q)}(\bar{\mathbf{x}}_2;\bar{\mathbf{y}}|p_2)\,G^{c\bar{c}_1}_{(g)}(\bar{\mathbf{x}}_g;\bar{\mathbf{y}}|\omega)\,T^{\bar{c}_1}_{\bar{b}_1\bar{a}_1}\,G^{\bar{a}_1a}_{(q)}(\bar{\mathbf{y}};\bar{\mathbf{x}}_1|p_1)$$
$$\times e^{i\mathbf{p}_{1\perp}\cdot(\mathbf{x}_1-\bar{\mathbf{x}}_1)-i\mathbf{p}_{2\perp}\cdot(\mathbf{x}_2-\bar{\mathbf{x}}_2)-i\mathbf{k}_\perp\cdot(\mathbf{x}_g-\bar{\mathbf{x}}_g)}\,. \quad (2.17)$$

The radiation probability (2.17) has a simple diagrammatic representation in configuration space which we give in Fig. 2. We denote by solid lines the full quark Greens's functions $G_{(q)}$, and by dashed lines the gluon Green's functions $G_{(g)}$. Contributions to the amplitude are on the l.h.s., those to the complex conjugate amplitude on the r.h.s. . We consider only the case that the gluon radiation occurs at larger longitudinal position in the complex conjugate amplitude, $\bar{y}^l>y^l$. Taking twice the real part in (2.17) accounts automatically for the other case. Transverse integration variables and colours are specified at the end points of the Green's functions. In this way, the simple diagram of Fig. 2 characterizes the rather lengthy expression (2.17) completely.

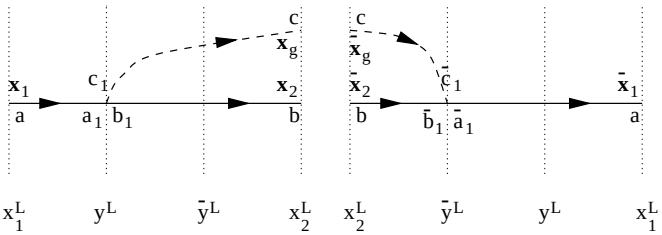

FIG. 2. Diagrammatic representation of the radiation probability (2.17) in configuration space. For details, see text.

The following sections are devoted to a study of the $\mathbf{k}_\perp$-differential gluon radiation cross section off a free incoming quark. From (2.17), we obtain

$$\frac{d^3\sigma^{(in)}}{d(\ln x)\,d\mathbf{k}_\perp}=\frac{\alpha_s}{(2\pi)^2}\,\frac{1}{4\,E_1^2\,(1-x)^2}\int d\mathbf{p}_\perp\,\langle|\mathcal{M}_{a\to b\,c}|^2\rangle$$
$$=C_{\mathrm{pre}}\,2\,\mathrm{Re}\int_{z_-}^{z_+}dy_l\int_{y_l}^{z_+}d\bar{y}_l\,e^{i\bar{q}(y_l-\bar{y}_l)-\epsilon\,|y_l|-\epsilon\,|\bar{y}_l|}$$
$$\times\int d\mathbf{y}\,d\bar{\mathbf{y}}\,d\mathbf{x}_1\,d\bar{\mathbf{x}}_1\,d\mathbf{x}_g\,d\bar{\mathbf{x}}_g\,d\mathbf{x}_2\,e^{-i\mathbf{k}_\perp\cdot(\mathbf{x}_g-\bar{\mathbf{x}}_g)}\,.$$
$$\times\Big\langle G^{aa_1}_{(q)}(\mathbf{x}_1;\mathbf{y}|p_1)\,T^{c_1}_{a_1b_1}\,\left(\frac{\partial}{\partial\mathbf{y}}G^{c_1c}_{(g)}(\mathbf{y};\mathbf{x}_g|\omega)\right)$$
$$\times G^{b_1b}_{(q)}(\mathbf{y};\mathbf{x}_2|p_2)\,G^{b\bar{b}_1}_{(q)}(\mathbf{x}_2;\bar{\mathbf{y}}|p_2)$$
$$\times\left(\frac{\partial}{\partial\bar{\mathbf{y}}}G^{c\bar{c}_1}_{(g)}(\bar{\mathbf{x}}_g;\bar{\mathbf{y}}|\omega)\right)\,T^{\bar{c}_1}_{\bar{b}_1\bar{a}_1}\,G^{\bar{a}_1a}_{(q)}(\bar{\mathbf{y}};\bar{\mathbf{x}}_1|p_1)\Big\rangle\,, \quad (2.18)$$

where

$$C_{\mathrm{pre}}=\frac{\alpha_s}{(2\pi)^2}\,\frac{1}{x^2\,E_1^2\,(1-x)^2} \quad (2.19)$$

accounts for a combination of recurring kinematical factors. Expression (2.18) is given in the frame in which the incoming quark has vanishing transverse momentum $\mathbf{p}_{1\perp}=0$. The medium average $\langle\ldots\rangle$ over the colours and positions of the scattering centers is specified in section II A below. In appendix B, we give details of why the combination of interaction vertices (2.16) can be writ-

ten to leading order in $O(x)$ as derivatives acting on the gluon Green's functions.

A. Medium average

The main tool of our analysis of the radiation cross section (2.18) will be an expansion of the Green's functions in powers of the scattering potential A_0:

$$\begin{aligned} G(\mathbf{r},z;\mathbf{r}',z'|p) &\equiv G_0(\mathbf{r},z;\mathbf{r}',z'|p) - i\int_z^{z'} d\xi \\ &\times \int d\boldsymbol{\rho}\, G_0(\mathbf{r},z;\boldsymbol{\rho},\xi|p)\, A_0(\boldsymbol{\rho},\xi)\, G_0(\boldsymbol{\rho},\xi;\mathbf{r}',z'|p) \\ &+\mathcal{P}\int_{z_L}^{x_L} d\xi_1 \int_{\xi_1}^{x_L} d\xi_2 \int d\boldsymbol{\rho}_1\, d\boldsymbol{\rho}_2\, G_0(\mathbf{r},z;\boldsymbol{\rho}_1,\xi_1|p) \\ &\times i\, A_0(\boldsymbol{\rho}_1,\xi_1)\, G_0(\boldsymbol{\rho}_1,\xi_1;\boldsymbol{\rho}_2,\xi_2|p) \\ &\times i\, A_0(\boldsymbol{\rho}_2,\xi_2)\, G(\boldsymbol{\rho}_2,\xi_2;\mathbf{r}',z'|p)\,. \end{aligned} \tag{2.20}$$

Here, G_0 is the free non-interacting Green's function

$$G_0(\mathbf{r},z;\mathbf{r}',z'|p) \equiv \frac{p}{2\pi i(z'-z)} \exp\left\{\frac{ip\,(\mathbf{r}-\mathbf{r}')^2}{2(z'-z)}\right\}, \tag{2.21}$$

and the only distinction between the quark and gluon Green's function lies in the colour representation of the spatially extended colour potential A_0. An expansion of the radiation cross section (2.18) to order $O(A_0^{2n})$ will turn out to be an expansion to n-th order in the opacity of the medium [12, 19]. Accordingly, we shall refer to (2.20) as opacity expansion.

We now discuss the calculation of the medium average in (2.18) to fixed order in opacity. To this end, we write for a single scattering potential, centered at $(\check{\mathbf{r}}_i,\check{z}_i)$,

$$\begin{aligned} \varphi_i^a(\mathbf{x}_\perp,\xi) = \delta^{a\,a_i} \int \frac{d^3\boldsymbol{q}}{(2\pi)^3}\, a_0(\boldsymbol{q}_\perp) \\ \times e^{-i(\mathbf{x}_\perp-\check{\mathbf{r}}_i)\cdot\boldsymbol{q}_\perp} e^{-i(\xi-\check{z}_i)q_l}\,. \end{aligned} \tag{2.22}$$

Here, the high-energy approximation $a_0(\boldsymbol{q}) \approx a_0(\boldsymbol{q}_\perp)$ implies that the effective momentum transfer occurs at fixed longitudinal position $\xi = \check{z}_i$. The medium average $\langle\ldots\rangle$ is the average over the transverse and longitudinal positions $(\check{\mathbf{r}}_i,\check{z}_i)$ of the scattering potentials and over the colours a_i exchanged with the i-th scattering center,

$$\begin{aligned} \langle f\rangle \equiv \frac{1}{A_\perp}\left(\prod_{i=1}^{N}\sum_{a_i}\int d\check{\mathbf{r}}_i\, d\check{z}_i\right) \\ \times f(\check{\mathbf{r}}_1,\ldots,\check{\mathbf{r}}_N;\check{z}_1,\ldots,\check{z}_N;a_1,\ldots,a_N)\,. \end{aligned} \tag{2.23}$$

$A_\perp$ is a total transverse area which we divide out to regain the cross section per unit transverse area. N is the number of different single scattering potentials up to which the function f is expanded.

To simplify notation, we replace in what follows the discrete sum over $\check{z}_i$ in (2.10) by an integral over the density n of scattering centers

$$A_0(\mathbf{x}_\perp,\xi) = \int d\check{z}_i\, n(\check{z}_i)\, \varphi_i^a(\mathbf{x}_\perp,\xi)\, T^a\,. \tag{2.24}$$

Since the effective momentum transfer from the single potential $\varphi_i^a(\mathbf{x}_\perp,\xi)$ occurs at $\xi = \check{z}_i$, we shall often work with ξ as integration variable.

B. Leading $O(x)$ approximation

We restrict our analysis of (2.18) to the kinematical region where the fraction x of the energy carried away by the gluon is small, $x \ll 1$. This $O(x)$ approximation is commonly used in the analysis of the abelian and non-abelian LPM-effect. It focusses on the kinematical region in which most of the radiation occurs. Technically, it allows for two important simplifications:

1. The leading $O(x)$ spin- and helicity-averaged product of the interaction vertices takes in momentum space the simple form

$$\hat{\Gamma}_{\mathbf{y}}\,\hat{\Gamma}^\dagger_{\bar{\mathbf{y}}} \longrightarrow \frac{4}{x^2}\,\mathbf{k}_{1\perp}\cdot\bar{\mathbf{k}}_{1\perp}\,, \tag{2.25}$$

   where $\mathbf{k}_{1\perp}$ and $\bar{\mathbf{k}}_{1\perp}$ are the transverse momenta of the gluon at the radiation vertex in the amplitude ($\mathbf{k}_{1\perp}$) and complex conjugate amplitude ($\bar{\mathbf{k}}_{1\perp}$). In configuration space, these momenta are conjugate to the $\mathbf{y}$-derivatives of the gluon Green's functions. Details are explained in appendix B.

2. Propagation of the transverse plane waves by Green's functions leads in (2.17) to the appearance of longitudinal phase factors:

$$\begin{aligned} &\int d\mathbf{x}_2\, G_0(\mathbf{x}_1,z_1;\mathbf{x}_2,z_2|E)\, e^{-i\,\mathbf{p}_\perp\cdot\mathbf{x}_2} \\ &= e^{-i\,\mathbf{p}_\perp\cdot\mathbf{x}_1}\,\exp\left[-i\frac{\mathbf{p}_\perp^2}{2\,E}\,(z_2-z_1)\right]. \end{aligned} \tag{2.26}$$

   To leading $O(x)$, the longitudinal phase receives only contributions from the transverse energy $\mathbf{p}_\perp^2/2\,\omega$ of the gluon. Transverse energies $\mathbf{p}_\perp^2/2\,E_1$ of the quarks are suppressed by one order in x. In this sense, the leading $O(x)$ approximation neglects the Brownian motion associated with the rescattering of the hard quark. Gluon rescattering is the dominant contribution, as observed by BDMPS.

III. OPACITY EXPANSION

For more than $N = 1$ scattering centers, the opacity expansion of the radiation cross section (2.18) involves non-vanishing interference terms between amplitudes of different powers in A_0. Two examples of non-vanishing interference effects between amplitudes of order $O(A_0)$ and $O(A_0^3)$ in the $N = 2$ opacity expansion are e.g.

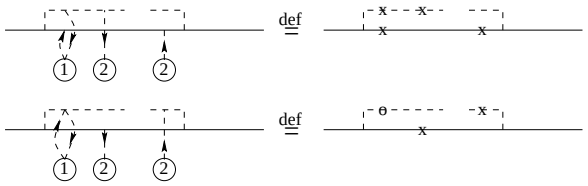

(3.1)

In what follows, we use the expression *contact term* to denote scattering centers which link with two gluons to one amplitude [as e.g. the first scattering center in (3.1)]. The notion *real term* characterizes a scattering center which exchanges one gluon with the amplitude and one with the complex conjugate amplitude [as does the second scattering center in (3.1)]. The structure of the medium average (2.23) ensures that all diagrammatic contributions are combinations of real and contact terms. For a medium of density $n(\xi)$ and thickness L, arbitrary combinations of N real and contact terms contribute to the same order $\left(\alpha_s \int_0^\infty n(\xi)\, d\xi\right)^N$ in opacity. Hence, contact term contributions cannot be neglected in the calculation of (2.18). Calculations which do not include contact terms [12, 17] describe an exclusive measurement in which the number of recoil target partons is determined. In section III A, we discuss the fundamental properties of contact terms as well as a set of identities which relate them to real terms. In section III B, we use these identities to derive a manifestly colour trivial expression (3.13) for the radiation cross section off N scattering centers. Then, we calculate (3.13) in an opacity expansion for $N = 1$ and $N = 2$.

A. Notation and identities

The medium average (2.23) ensures that contact terms do not transfer a net momentum to the final state. However, they can change the transverse momentum between the outgoing particles [19]. This can be seen, e.g., by writing for the first scattering center in (3.1) the corresponding contributions (2.22) and realizing that the medium average (2.23) results in a δ-function $\delta^{(2)}\left(\boldsymbol{q}_{1\perp} + \bar{\boldsymbol{q}}_{1\perp}\right)$ with the transverse momenta of both gluons appearing in the same amplitude.

Contact terms satisfy several important identities. All the following identities can be established by writing out the opacity expansion (2.20) for the last scattering center before the cut and employing the medium average (2.23). Several examples of this technique were discussed explicitly in [19]. Here, we consider diagrams to N-th order in opacity. We denote by a shaded box the longitudinal region in which the $N-1$ first interactions take place, and we specify the contribution of the last N-th scattering center explicitly. We start with the case that the last interaction links to the quark line. Irrespective of whether it occurs after $\bar{y}_l$,

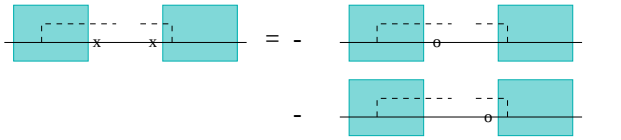

(3.2)

or before y_l,

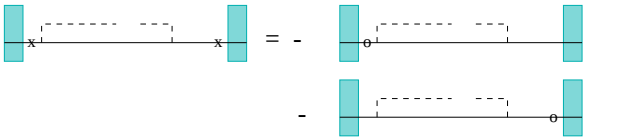

(3.3)

the real contribution equals in both cases minus the two corresponding contact terms and thus cancels against them. We note that (3.2) holds exactly. It is based on the identity derived in Fig. 7a of Ref. [19]. Equation (3.3), in contrast, involves the leading $O(x)$ approximation: the l.h.s. of (3.3) involves a phase $\exp\left[-i\frac{\mathbf{p}_\perp^2}{2\,p_1}(y_l - \bar{y}_l)\right]$ whose transverse momentum $\mathbf{p}_\perp^2$ differs by the amount $\boldsymbol{q}_{N\perp}$ of the last rescattering from the corresponding phase on the r.h.s. of (3.3). This phase does not contribute in the leading $O(x)$ approximation where the momentum transfer to the quark line is neglected and only transverse energies of the gluon are kept. The same argument allows for an identity concerning the first scattering center:

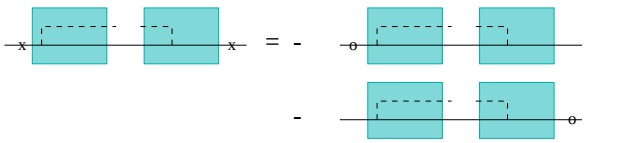

(3.4)

The important implication of this identity is that the sum of all rescattering contributions to (2.18) which have the first interaction before y_l, vanishes. This eliminates a large class of diagrams from our calculation.

In addition, there are identities in which one of the gluon lines is touched:

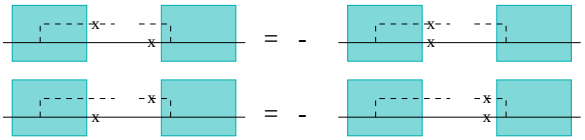

(3.5)

These identities are exact and were derived already in Fig. 7b of Ref. [19].

So far, we have discussed identities for which the last interaction occured either after $\bar{y}_l$ or before y_l. Now we give relations which hold for a last interaction at longitudinal position $y_l < \xi < \bar{y}_l$. These identities necessarily involve knowledge of the colour algebra. The simplest example is

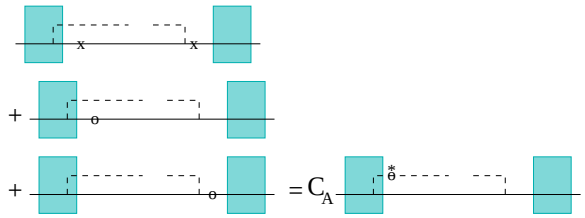

(3.6)

Here, the r.h.s. shows a star over the interaction term. This notation indicates an interaction term without colour factor. The colour information is absorbed in the prefactor of the diagram. To derive (3.6), we denote the colour generators of the left and right shaded blocks in (3.6) by factors L and R, respectively. The colour trace of the first term on the l.h.s. then takes the form

$$\mathrm{Tr}\,[L\,T_d\,T_c\,T_d\,R] = \left(C_F - \frac{C_A}{2}\right)\,\mathrm{Tr}\,[L\,T_c\,R]\;, \qquad (3.7)$$

where T_d is the generator associated with the N-th interaction and T_c that of the quark-gluon emission vertex at $\bar{y}_l$. The contact terms on the left and right hand side of (3.6) are proportional to $\mathrm{Tr}\,[L\,T_c\,R]$ with prefactors $-\frac{C_F}{2}$ and $-\frac{C_A}{2}$, respectively. In the leading $O(x)$ approximation, there is no complication from the momentum structure of the diagrams and equation (3.7) thus ensures the identity (3.6).

In a similar way, one can establish an identity for diagrams in which one of the interactions links to the gluon line:

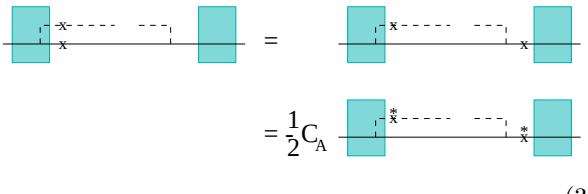

(3.8)

This is a direct consequence of the relation

$$i\,f_{\bar{c}dc}\,\mathrm{Tr}\,[L\,T_c\,T_d\,R] = \frac{1}{2}\,C_A\,\mathrm{Tr}\,[L\,T_{\bar{c}}\,R]\;. \qquad (3.9)$$

B. Colour triviality of the gluon radiation cross section

The identities of the last subsection have two important properties which we exploit systematically in what follows: (i) they allow for many diagrammatic cancellations between real and contact terms, and (ii) they ensure that the remaining terms combine to expressions which are proportional to C_A^N.

1. *Classification of diagrams*

In what follows, we consider all diagrammatic contributions which are N-th order in opacity. The $N-1$ first interaction terms are again summarized diagrammatically in a shaded block on both sides of the cut. The last interaction is specified explicitly. We consider three cases

Case I: The last interaction occurs at longitudinal position $\xi_N < y_l$.
In this case, the identity (3.2) ensures that the sum of all real and contact terms of the last interaction vanish.

Case II: The last interaction occurs at longitudinal position $y_l < \xi_N < \bar{y}_l$.
In this case, we have two real and four contact contributions from the last interaction. According to the identities (3.6) and (3.8), they add up in the following way:

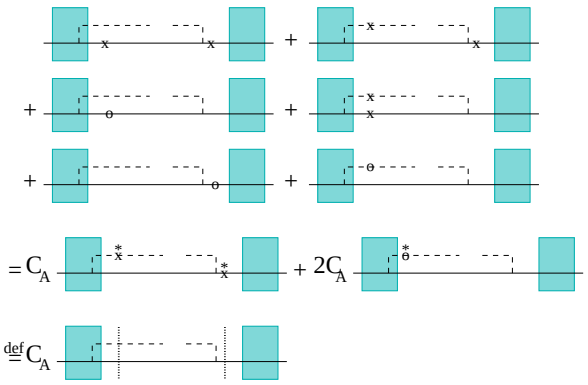

(3.10)

In the last line, we have introduced a simple shorthand which summarizes all non-vanishing contributions for $y_l < \xi_N < \bar{y}_l$. For what follows, it is important that this shorthand comes with a unique colour prefactor C_A which absorbs the colour algebra of the last interaction.

Case III: The last interaction occurs at longitudinal position $\bar{y}_l < \xi_N$.
In this case, we have four real and six contact term contributions. Identity (3.2) ensures that the one real and two contact terms shown there cancel each other. Identity (3.5) leads to the cancellation of two real versus two

contact terms. For the remaining one real and two contact terms, we introduce the notational shorthand:

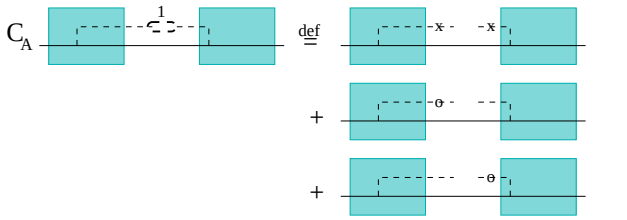

(3.11)

Again, the sum of all non-vanishing contributions comes with a colour prefactor C_A which absorbs the colour algebra of the last interaction.

2. Iteration

The above classification of diagrams shows that the colour structure of all surviving contributions to the last N-th interaction can be absorbed in a prefactor C_A. This allows for an iteration of the above procedure to the earlier $(N-1)$-th, $(N-2)$-th, $(N-3)$-th etc. interactions.

We consider first the case that the m last interactions occur at positions larger $\bar{y}_l$, i.e., $\bar{y}_l < \xi_{N-m} < \xi_{N-m+1} < \ldots < \xi_N$. For the N-th interaction, we are left with the diagrams of (3.11). Since the colour structure is absorbed in the prefactor C_A, the arguments leading to (3.11) apply also to the $(N-1)$-th interaction. If the $(N-(m+1))$-th interaction also occurs after $\bar{y}_l$, then the sum of all nonvanishing contributions is given by the recursively defined diagram

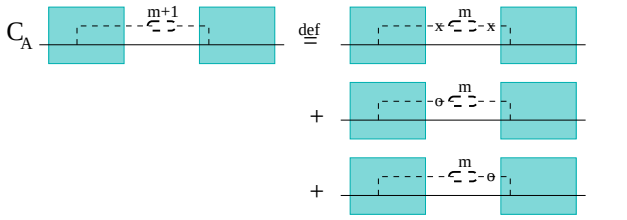

(3.12)

For N-fold rescattering, an arbitrary number $m < N$ interactions will occur after $\bar{y}_l$, the remaining $(N-m)$ interactions will occur at longitudinal positions between y_l and $\bar{y}_l$. The contributions of all possible diagrams with interactions before y_l cancels due to the identity (3.4). The radiation cross section (2.18) to N-th order in opacity can thus be represented in the compact diagrammatic and explicitly colour trivial form

$$\frac{d^3\sigma^{(in)}(N)}{d(\ln x)\,d\mathbf{k}_\perp} = \frac{\alpha_s}{(2\pi)^2}\,\frac{1}{\omega^2}\,N_C\,C_F\,C_A^N \tag{3.13}$$

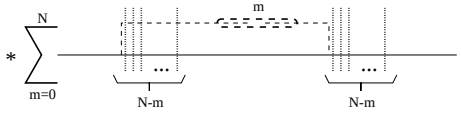

This is the diagrammatic manifestation of the observation of BDMPS that gluon rescattering alone gives the leading $O(x)$ contribution to the radiation cross section (2.18). As can be seen from (3.10) and (3.12), all N scattering centers involved transfer momentum to the gluon line.

We introduce for the diagrammatic part of (3.13) an analytical shorthand

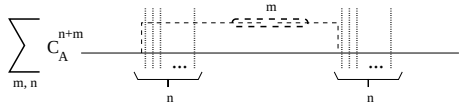

$$\begin{aligned}
&= \int_Y \int_{[q_i,\xi_i]_{i\in[1,N]}} \int d\mathbf{y}\,d\bar{\mathbf{y}}\,d\mathbf{s}\,d\mathbf{x}_g\,d\bar{\mathbf{x}}_g \\
&\quad\times \left(\frac{\partial}{\partial \mathbf{y}}\tilde{G}(\mathbf{y};\mathbf{x}_g|\omega)\right) e^{-i\mathbf{k}_\perp\cdot\mathbf{x}_g}\,\tilde{G}_0(\mathbf{y};\bar{\mathbf{y}}|p_2) \\
&\quad\times e^{i\mathbf{k}_\perp\cdot\bar{\mathbf{x}}_g}\left(\frac{\partial}{\partial \bar{\mathbf{y}}}\tilde{G}(\bar{\mathbf{x}}_g;\bar{\mathbf{y}}|\omega)\right)\tilde{G}(\bar{\mathbf{y}},\bar{y}_l;\mathbf{s},y_l|p_1)\,.
\end{aligned} \tag{3.14}$$

To specify our notation, we compare (3.13) and (3.14) to the full radiation cross section (2.18). The term $\frac{\alpha_s}{(2\pi)^2}\frac{1}{\omega^2}$ in (3.13) is the leading order $O(x)$ of the prefactor $C_{\rm pre}$. The colour algebra of (2.18) simplifies to the Casimir factors in (3.13). Accordingly, the functions $\tilde{G}$ introduced in (3.14) are abelian. Some quark Green's functions in the diagram of (3.14) are non-interacting to arbitrary orders in opacity. This allows to integrate over $\mathbf{x}_1$, $\bar{\mathbf{x}}_1$ and $\mathbf{x}_2$ in (2.18). The new integration variable $\mathbf{s}$ in (3.14) denotes the transverse coordinate of the quark at longitudinal position y_l in the complex conjugate amplitude. The longitudinal y_l- and $\bar{y}_l$-integrals in (2.18) are given by the notational shorthand

$$\int_Y f \equiv 2\mathrm{Re}\int_{z_-}^{z_+} dy_l \int_{y_l}^{z_+} d\bar{y}_l\, e^{-\epsilon|y_l|-\epsilon|\bar{y}_l|}\,f\,, \tag{3.15}$$

where the function f denotes an unspecified integrand. To N-th order in opacity, the medium average $\langle\ldots\rangle$ in (2.18) results in N transverse momentum $\boldsymbol{q}_{i\perp}$-integrals,

$$\int_{q_i} f \equiv \int \frac{d\boldsymbol{q}_{i\perp}}{(2\pi)^2}|a_0(\boldsymbol{q}_{i\perp})|^2\,f\,, \tag{3.16}$$

which average over the elastic scattering cross sections $|a_0(\boldsymbol{q}_{i\perp})|^2$ for each scattering center. Also, it leads to N integrals over the allowed longitudinal positions $\xi_i \in [\xi_i^{\min},\xi_i^{\max}]$ of these N scattering centers,

$$\int_{\xi_i} f \equiv \int_{\xi_i^{\min}}^{\xi_i^{\max}} d\xi_i\,n(\xi_i)\,f\,. \tag{3.17}$$

These integrations are combined in (3.14) into

$$\int_{[q_i,\xi_i]_{i\in[1,N]}} f = \prod_{i=1}^{N}\int_{q_i}\int_{\xi_i} f\,. \tag{3.18}$$

As a consequence of factorizing in (2.18) the colour algebra, the elastic cross sections $|a_0(\boldsymbol{q}_{i\perp})|^2$ and the longitudinal momentum integrals over ξ_i, the only remnants of the opacity expansion (2.20) which are left in the integrand of (3.14) are transverse phase factors. Hence, the functions $\tilde{G}$ are defined by replacing in (2.20) $A_0(\boldsymbol{\rho},\xi_i) \to e^{-i\boldsymbol{q}_{i\perp}\cdot\boldsymbol{\rho}}$. For each $\boldsymbol{q}_{i\perp}$, two phases appear in the integrand of (3.14), one being the complex conjugate of the other. To gain familiarity with (3.14), one may consider simple examples like

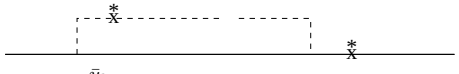

$$
\begin{aligned}
&= \int_Y \frac{1}{A_\perp} \int_{q_1} \int_{y_l}^{\bar{y}_l} d\xi_1\, n(\xi_1) \int d\mathbf{y}\, d\bar{\mathbf{y}}\, d\mathbf{s}\, d\mathbf{x}_g\, d\bar{\mathbf{x}}_g \\
&\times \left(\frac{\partial}{\partial \mathbf{y}} \int d\boldsymbol{\rho}_1 G_0(\mathbf{y};\boldsymbol{\rho}_1,\xi_1|\omega)\, e^{-i\boldsymbol{q}_{1\perp}\cdot\boldsymbol{\rho}_1}\, G_0(\boldsymbol{\rho}_1,\xi_1;\mathbf{x}_g|\omega) \right) \\
&\times e^{-i\mathbf{k}_\perp\cdot(\mathbf{x}_g-\bar{\mathbf{x}}_g)}\, G_0(\mathbf{y};\bar{\mathbf{y}}|p_2) \left(\frac{\partial}{\partial \bar{\mathbf{y}}} G_0(\bar{\mathbf{x}}_g;\bar{\mathbf{y}}|\omega) \right) \\
&\times \int d\bar{\boldsymbol{\rho}}_1 G_0(\bar{\mathbf{y}};\bar{\boldsymbol{\rho}}_1,\xi_1|p_1)\, e^{i\boldsymbol{q}_{1\perp}\cdot\bar{\boldsymbol{\rho}}_1}\, G_0(\bar{\boldsymbol{\rho}}_1,\xi_1;\mathbf{s},\bar{y}_l|p_1)\,, \\
&= \int_Y \int_{q_1} (\mathbf{k}_\perp + \boldsymbol{q}_{1\perp})\cdot\mathbf{k}_\perp \int_{y_l}^{\bar{y}_l} d\xi_1\, n(\xi_1) \\
&\quad \times e^{-i\frac{\mathbf{k}_\perp^2}{2\omega}(\bar{y}_l-\xi_1) - i\frac{(\mathbf{k}_\perp+\boldsymbol{q}_{1\perp})^2}{2\omega}(\xi_1-y_l)}\,. \qquad (3.19)
\end{aligned}
$$

Here, we have used again the leading $O(x)$ approximation to neglect the subleading contributions to the longitudinal phase of the integrand.

All N-th order contributions to the radiation spectrum (3.13) can be written as a sum of products of the form

$$
\begin{aligned}
\frac{d^3\sigma^{(in)}(N)}{d(\ln x)\, d\mathbf{k}_\perp} &= \frac{\alpha_s}{(2\pi)^2}\, \frac{1}{\omega^2}\, N_C\, C_F\, C_A^N \\
&\times \int_{q_1} \dots \int_{q_N} \sum_i \Gamma_{(i)}\, \mathcal{Z}_{(i)}\,. \qquad (3.20)
\end{aligned}
$$

Here, the factor

$$
\mathcal{Z}_{(i)} = \int_Y \Phi_{(i)}(y_l,\bar{y}_l)\,. \qquad (3.21)
$$

denotes an integral over longitudinal phase factors. To leading $O(x)$, this phase is obtained by iterative use of (2.26). The factor $\Phi_{(i)}$ in (3.21) is the integral of this phase over the allowed longitudinal position of scattering centers times a factor $-1/2$ for each contact term linking to the gluon line. In the example (3.19), $\Phi_{(i)}$ is given by the ξ_1-integral.

The factors $\Gamma_{(i)}$ in (3.20) denote the results of the partial derivatives in (3.14) for the i-th diagrammatic contribution. They are easily read off from the diagrams by adding up the momentum transfers to the gluon line in both amplitudes. For the example (3.19), this leads to the factor $(\mathbf{k}_\perp + \boldsymbol{q}_{1\perp})\cdot\mathbf{k}_\perp$. We now turn to an evaluation of (3.13) in the low opacity expansion for $N = 1$ and $N = 2$. In section IV, we derive then an all-order expression (4.15) for this radiation cross section. As explained in sections V and VI, this all order expression gives a much simpler access to the opacity expansion since it involves only $N + 1$ terms to N-th order.

C. $N = 1$ Gunion-Bertsch radiation spectrum

Here, we derive the Gunion-Bertsch radiation spectrum [22] as the $N = 1$ term in the opacity expansion of (3.13). This provides a first consistency check for our formalism and allows for a simple illustration of our diagrammatic rules. The N = 1-term of (3.13) has four contributions

$$
\begin{aligned}
\frac{d^3\sigma^{(in)}(N=1)}{d(\ln x)\, d\mathbf{k}_\perp} &= \frac{\alpha_s}{(2\pi)^2}\, \frac{1}{\omega^2}\, N_C\, C_F\, C_A \\
&\times \Big(\quad (1) \quad + 2 \quad (3) \\
&+ \quad (2) \quad + 2 \quad (4) \Big) \\
&= \frac{\alpha_s}{(2\pi)^2}\, \frac{1}{\omega^2}\, N_C\, C_F\, C_A \sum_{i=1}^{4} \Gamma_{(i)}\, \mathcal{Z}_{(i)}\,. \qquad (3.22)
\end{aligned}
$$

Here, we have labelled the different diagrammatic contributions by (1) - (4). Our diagrammatic rules distinguish between interactions before and after $\bar{y}_l$. For that reason, the diagrams (3) and (4) are both included in (3.22). Contribution (2) is the example studied in (3.19). The Γ-factors are read off from the i-th diagramm by adding up the transverse momentum flows into the gluon line on both sides of the cut:

$$
\Gamma_{(1)} = (\mathbf{k}_\perp + \boldsymbol{q}_{1\perp})\cdot(\mathbf{k}_\perp + \boldsymbol{q}_{1\perp}) \qquad (3.23)
$$

$$
\Gamma_{(2)} = (\mathbf{k}_\perp + \boldsymbol{q}_{1\perp})\cdot\mathbf{k}_\perp \qquad (3.24)
$$

$$
\Gamma_{(3)} = \Gamma_{(4)} = \mathbf{k}_\perp\cdot\mathbf{k}_\perp \qquad (3.25)
$$

For the leading $O(x)$ contributions to the factors $\mathcal{Z}_{(i)}$ in (3.19), only the transverse momenta of the gluon have to be considered. In (3.22), the gluon line comes with two possible transverse energies

$$
Q = \frac{\mathbf{k}_\perp^2}{2\omega}\,, \qquad Q_1 = \frac{(\mathbf{k}_\perp + \boldsymbol{q}_{1\perp})^2}{2\omega}\,. \qquad (3.26)
$$

Including a factor $-1/2$ for each contact term linking twice to the gluon line, we find for the phase factors $\Phi_{(i)}$

$$
\Phi_{(1)}(y_l,\bar{y}_l) = \int_{\bar{y}_l}^{z_+} d\xi\, n(\xi)\, e^{-iQ_1(\bar{y}_l-y_l)}\,, \qquad (3.27)
$$

$$
\Phi_{(2)}(y_l,\bar{y}_l) = \int_{y_l}^{\bar{y}_l} d\xi\, n(\xi)\, e^{-iQ(\bar{y}_l-\xi)-iQ_1(\xi-y_l)}\,, \qquad (3.28)
$$

$$
\Phi_{(3)}(y_l,\bar{y}_l) = -\int_{\bar{y}_l}^{z_+} d\xi\, n(\xi)\, e^{-iQ(\bar{y}_l-y_l)}\,, \qquad (3.29)
$$

$$
\Phi_{(4)}(y_l,\bar{y}_l) = -\int_{y_l}^{\bar{y}_l} d\xi\, n(\xi)\, e^{-iQ(\bar{y}_l-y_l)}\,. \qquad (3.30)
$$

For a homogeneous density distribution $n(\xi) = n_0$ of a medium of thickness L, the corresponding factors $\mathcal{Z}_{(i)}$ given in (3.21) are

$$\mathcal{Z}_{(1)} = \frac{L\, n_0}{Q_1^2}\,, \qquad \mathcal{Z}_{(2)} = \frac{-2\, L\, n_0}{Q\, Q_1}\,,$$
$$\mathcal{Z}_{(3)} = \frac{2\, L\, n_0}{Q^2}\,, \qquad \mathcal{Z}_{(4)} = \frac{-L\, n_0}{Q^2}\,. \tag{3.31}$$

Inserting this into the last line of (3.22), we find

$$\frac{d^3\sigma^{(in)}(N=1)}{d(\ln x)\, d\mathbf{k}_\perp} = \frac{\alpha_s}{\pi^2}\, (Ln_0)\, N_c C_F C_A \times \int_{q_1} \frac{\boldsymbol{q}_{1\perp}^2}{\mathbf{k}_\perp^2\, (\boldsymbol{q}_{1\perp}+\mathbf{k}_\perp)^2}\,. \tag{3.32}$$

This is the leading $O(x)$ contribution to the Gunion-Bertsch [22] radiation cross section times the opacity $L\, n_0$ of a homogeneous medium of thickness L.

D. $N = 2$ Opacity expansion

Before turning in the next section to a systematic all-order analysis of the radiation cross section (3.13), we calculate here the $N = 2$ contribution to the opacity expansion.

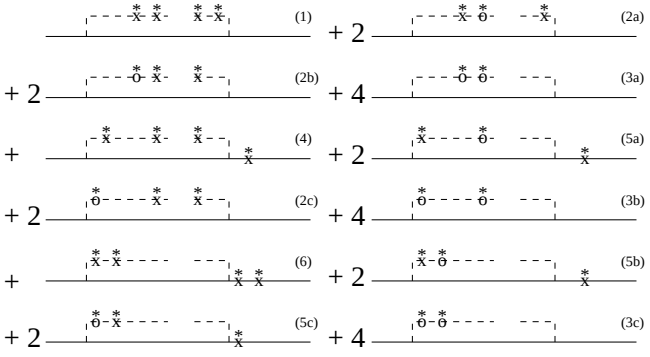

FIG. 3. All non-vanishing contributions to the $N = 2$ radiation cross section as given by (3.13). Diagrams are labelled with a double index (ix), see text for details.

All terms contributing to the $N = 2$ contribution of (3.13) are listed in Fig. 3. We have labelled them with a double index (ix). The first index $i = 1, 2, \ldots, 6$ indicates how the diagram contributes to the interaction vertex (2.25),

$$\Gamma_{(1)} = (\mathbf{k}_\perp + \boldsymbol{q}_{1\perp} + \boldsymbol{q}_{2\perp})^2\,, \tag{3.33}$$
$$\Gamma_{(2)} = (\mathbf{k}_\perp + \boldsymbol{q}_{1\perp})^2\,, \tag{3.34}$$
$$\Gamma_{(3)} = \mathbf{k}_\perp^2\,, \tag{3.35}$$
$$\Gamma_{(4)} = (\mathbf{k}_\perp + \boldsymbol{q}_{1\perp} + \boldsymbol{q}_{2\perp}) \cdot (\mathbf{k}_\perp + \boldsymbol{q}_{1\perp})\,, \tag{3.36}$$
$$\Gamma_{(5)} = (\mathbf{k}_\perp + \boldsymbol{q}_{1\perp}) \cdot \mathbf{k}_\perp\,, \tag{3.37}$$
$$\Gamma_{(6)} = (\mathbf{k}_\perp + \boldsymbol{q}_{1\perp} + \boldsymbol{q}_{2\perp}) \cdot \mathbf{k}_\perp\,. \tag{3.38}$$

The integration variables $\boldsymbol{q}_{1\perp}$ and $\boldsymbol{q}_{2\perp}$ for the first and second momentum transfer can be relabelled freely. As a consequence, we have to consider only three different transverse gluon energies

$$Q = \frac{\mathbf{k}_\perp^2}{2\omega}\,, \qquad Q_1 = \frac{(\mathbf{k}_\perp + \boldsymbol{q}_{1\perp})^2}{2\omega}\,,$$
$$Q_2 = \frac{(\mathbf{k}_\perp + \boldsymbol{q}_{1\perp} + \boldsymbol{q}_{2\perp})^2}{2\omega}\,, \tag{3.39}$$

and no term $\propto (\mathbf{k}_\perp + \boldsymbol{q}_{2\perp})$ appears in the interaction vertices (3.33)-(3.38).

The phase factors can be read off from the diagrams of Fig. 3 as described above. They are now integrals over the allowed positions ξ_1 and ξ_2 of both scattering centers, e.g.,

$$\Phi_{(6)}(y_l, \bar{y}_l) = \int_{y_l}^{\bar{y}_l} d\xi_1 \int_{\xi_1}^{\bar{y}_l} d\xi_2\, n(\xi_1)\, n(\xi_2) \times e^{-iQ(\bar{y}_l - \xi_2) - iQ_1(\xi_2 - \xi_1) - iQ_2(\xi_1 - y_l)}\,. \tag{3.40}$$

The second index $x = a, b, \ldots$ labels in Fig. 3 the different diagrammatic contributions to the same term $\Gamma_{(i)}$. Denoting by the phases $\Phi_{(i)}$ the sum over all contributions (e.g. $\Phi_{(3)} = \Phi_{(3a)} + \Phi_{(3b)} + \Phi_{(3c)}$), we find for the factors $\mathcal{Z}_{(i)}$ according to (3.21)

$$\mathcal{Z}_{(1)} = \frac{L^2}{2\, Q_2^2}\, n_0^2\,, \tag{3.41}$$
$$\mathcal{Z}_{(2)} = \frac{-2 + 2\, \cos(L\, Q_1)}{Q_1^4}\, n_0^2\,, \tag{3.42}$$
$$\mathcal{Z}_{(3)} = \frac{-L^2}{2\, Q^2}\, n_0^2\,, \tag{3.43}$$
$$\mathcal{Z}_{(4)} = \frac{2 - 2\, \cos(L\, Q_1) - L^2\, Q_1^2}{Q_1^3\, Q_2}\, n_0^2\,, \tag{3.44}$$
$$\mathcal{Z}_{(5)} = \frac{2 - 2\, \cos(L\, Q_1) + L^2\, Q_1^2}{Q_1^3\, Q}\, n_0^2\,, \tag{3.45}$$
$$\mathcal{Z}_{(6)} = \frac{-2 + 2\, \cos(L\, Q_1)}{Q\, Q_1^2\, Q_2}\, n_0^2\,. \tag{3.46}$$

These terms are multiplied by a factor $-1/2$ for each contact term linking twice to the gluon line. The corresponding radiation cross section (3.20) shows L-dependent oscillations which are due to the interference between the gluon radiation of the two spatially separated scattering centers. We consider especially for fixed opacity $L\, n_0$ the limits $L \to 0$ and $L \to \infty$ in which the two scattering centers sit on top of each other and at arbitrary large separation, respectively. We find

$$\lim_{L\to\infty} \left.\frac{d^3\sigma^{(in)}(N=2)}{d(\ln x)\, d\mathbf{k}_\perp}\right|_{L\, n_0 = \text{fixed}} = \frac{\alpha_s}{\pi^2}\, N_c\, C_F\, C_A^2\, \frac{(Ln_0)^2}{2} \times \int_{q_1} \int_{q_2} \left[R(\mathbf{k}_\perp + \boldsymbol{q}_{1\perp}, \boldsymbol{q}_{2\perp}) - R(\mathbf{k}_\perp, \boldsymbol{q}_{1\perp})\right]\,, \tag{3.47}$$

and

$$\lim_{L\to 0}\left.\frac{d^3\sigma^{(in)}(N=2)}{d(\ln x)\,d\mathbf{k}_\perp}\right|_{L\,n_0=\text{fixed}} = \frac{\alpha_s}{\pi^2}\,N_c\,C_F\,C_A^2\,\frac{(Ln_0)^2}{2}$$
$$\times\int_{q_1}\int_{q_2}\left[R(\mathbf{k}_\perp,\boldsymbol{q}_{1\perp}+\boldsymbol{q}_{2\perp})-2\,R(\mathbf{k}_\perp,\boldsymbol{q}_{1\perp})\right]. \quad (3.48)$$

We have written these limiting cases in terms of the momentum-dependent part R of the Gunion-Bertsch QCD radiation spectrum (3.22),

$$R(\mathbf{k}_\perp,\boldsymbol{q}_\perp)=\frac{\boldsymbol{q}_\perp^2}{\mathbf{k}_\perp^2\,(\mathbf{k}_\perp+\boldsymbol{q}_\perp)^2}, \quad (3.49)$$

which is associated to a quark of transverse momentum $\mathbf{k}_\perp$, receiving a momentum transfer $\boldsymbol{q}_\perp$ in the scattering.

One may expect that in the coherent factorization limit $L\to 0$, the radiation spectrum corresponds to one single Gunion-Bertsch term $R(\mathbf{k}_\perp,\boldsymbol{q}_{1\perp}+\boldsymbol{q}_{2\perp})$ with effective momentum transfer $(\boldsymbol{q}_{1\perp}+\boldsymbol{q}_{2\perp})$, and that in the incoherent limit $L\to\infty$ (which for QCD is of course only of formal interest), the radiation cross section is the sum of two independent Gunion-Bertsch terms. The results (3.48) and (3.49) differ from these expectations by the term

$$-\frac{\alpha_s}{\pi^2}\,N_c\,C_F\,C_A^2\,\frac{(Ln_0)^2}{2}\int_{q_1}\int_{q_2}2\,R(\mathbf{k}_\perp,\boldsymbol{q}_{1\perp}). \quad (3.50)$$

The origin of this term will be explained in section V.

IV. A PATH-INTEGRAL FOR ARBITRARY ORDERS IN OPACITY

In this section, we derive a path-integral representation for the radiation cross section (3.13) which is valid to arbitrary orders in opacity. We start from (3.14), summed over powers of opacity:

$$\sum_{m,\,n} C_A^{n+m}$$

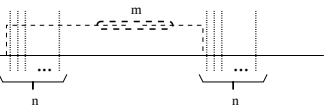

$$=\frac{1}{A_\perp}\int_Y\int d\mathbf{y}\,d\bar{\mathbf{y}}\,d\mathbf{s}\,d\mathbf{u}\left(\frac{\partial}{\partial\bar{\mathbf{y}}}F(\mathbf{u}-\bar{\mathbf{y}})\right)$$
$$\times\frac{\partial}{\partial\mathbf{r}_3(y_l)}M(\mathbf{r}_1,\mathbf{r}_2,\mathbf{r}_3|y_l,\bar{y}_l). \quad (4.1)$$

We have separated in this expression scattering contributions from longitudinal positions before and after $\bar{y}_l$. The integration variables $\mathbf{u}$ and $\bar{\mathbf{y}}$ denote the transverse positions of the gluon at $\bar{y}_l$ in the amplitude and complex conjugate amplitude, respectively. All contributions in the region $y_l<\xi<\bar{y}_l$ are given by

$$M(\mathbf{r}_1,\mathbf{r}_2,\mathbf{r}_3|y_l,\bar{y}_l)=\sum_{n=0}^{\infty}C_A^n\int_{[q_i,\xi_i]_{i\in[1,n]}}$$
$$\times\tilde{G}(\mathbf{r}_3(y_l),y_l;\mathbf{r}_3(\bar{y}_l),\bar{y}_l|\omega)$$
$$\times G_0(\mathbf{r}_2(y_l),y_l;\mathbf{r}_2(\bar{y}_l),\bar{y}_l|p_2)$$
$$\times\tilde{G}(\mathbf{r}_1(\bar{y}_l),\bar{y}_l;\mathbf{r}_1(y_l),y_l|p_1), \quad (4.2)$$

where the transverse paths $\mathbf{r}_i(\xi)$, $i\in[1,3]$, satisfy the boundary conditions

$$\mathbf{r}_1(y_l)=\mathbf{s}, \qquad \mathbf{r}_1(\bar{y}_l)=\bar{\mathbf{y}}, \quad (4.3)$$
$$\mathbf{r}_2(y_l)=\mathbf{y}, \qquad \mathbf{r}_2(\bar{y}_l)=\bar{\mathbf{y}}, \quad (4.4)$$
$$\mathbf{r}_3(y_l)=\mathbf{y}, \qquad \mathbf{r}_3(\bar{y}_l)=\mathbf{u}. \quad (4.5)$$

The contributions coming from longitudinal positions $\xi>\bar{y}_l$ are summarized by the function

$$F(\mathbf{u}-\bar{\mathbf{y}})=\sum_{m=0}^{\infty}C_A^m\int_{[q_i,\xi_i]_{i\in[1,m]}}\int d\mathbf{x}_g\,d\bar{\mathbf{x}}_g$$
$$\times\tilde{G}(\mathbf{u},\bar{y}_l;\mathbf{x}_g,z_+|\omega)\,e^{-i\mathbf{k}_\perp\cdot(\mathbf{x}_g-\bar{\mathbf{x}}_g)}$$
$$\times\tilde{G}(\bar{\mathbf{x}}_g,z_+;\bar{\mathbf{y}},\bar{y}_l|\omega). \quad (4.6)$$

Here, we have anticipated that the function F depends only on the difference $\mathbf{u}-\bar{\mathbf{y}}$ of the two integration variables $\mathbf{u}$ and $\bar{\mathbf{y}}$. The consistency of our starting point (4.1) with the rescattering part to the radiation cross section (3.13) is straightforward to check by inserting (4.2)-(4.6) into (4.1).

In what follows, we discuss how to simplify (4.2) and (4.6) in terms of the dipole cross section

$$\sigma(\boldsymbol{\rho})=2\,C_A\int\frac{d\boldsymbol{q}_\perp}{(2\pi)^2}\,|a_0(\boldsymbol{q}_\perp)|^2\left(1-e^{-i\boldsymbol{q}_\perp\cdot\boldsymbol{\rho}}\right). \quad (4.7)$$

1. Gluon rescattering for $\xi>\bar{y}_l$

We start with the analysis of the function F in (4.6) which describes the gluon rescattering at longitudinal positions $\xi>\bar{y}_l$. The first order term $m=1$ reads

$$=C_A\int_{\bar{y}_l}^{z_+}d\xi_1\,n(\xi_1)\int\frac{d\boldsymbol{q}_\perp}{(2\pi)^2}\,|a_0(\boldsymbol{q}_\perp)|^2$$
$$\times\int d\mathbf{x}_g\,d\bar{\mathbf{x}}_g\,e^{-i\mathbf{k}_\perp\cdot(\mathbf{x}_g-\bar{\mathbf{x}}_g)}\int d\mathbf{r}(\xi_1)\,d\bar{\mathbf{r}}(\xi_1)$$
$$\times G_0(\mathbf{u},\bar{y}_l;\mathbf{r}(\xi_1)|\omega)\,G_0(\mathbf{r}(\xi_1);\mathbf{x}_g,z_+|\omega)$$
$$\times G_0(\bar{\mathbf{x}}_g,z_+;\bar{\mathbf{r}}(\xi_1)|\omega)\,G_0(\bar{\mathbf{r}}(\xi_1);\bar{\mathbf{y}},\bar{y}_l|\omega)$$
$$\times\left(e^{-i\boldsymbol{q}(\mathbf{r}(\xi_1)-\bar{\mathbf{r}}(\xi_1))}-1\right) \quad (4.8)$$
$$=-\frac{1}{2}\int_{\bar{y}_l}^{z_+}d\xi_1\,n(\xi_1)\,\sigma(\mathbf{u}-\bar{\mathbf{y}})\;e^{-i\mathbf{k}_\perp\cdot(\mathbf{u}-\bar{\mathbf{y}})}, \quad (4.9)$$

The factors in the last line of (4.8) correspond to the three terms on the right hand side of (3.11) and can be combined to a dipole cross section (4.7). It is straightforward to iterate this relation

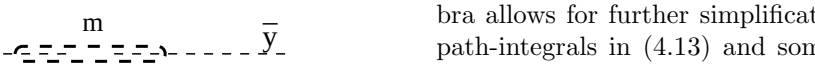

$$= \frac{1}{m!}\left(-\frac{1}{2}\int_{\bar{y}_l}^{z_+} d\xi\, n(\xi)\,\sigma\left(\mathbf{u}-\bar{\mathbf{y}}\right)\right)^m e^{-i\mathbf{k}_\perp\cdot(\mathbf{u}-\bar{\mathbf{y}})}\,. \quad (4.10)$$

Here, the prefactor $\frac{1}{m!}$ stems from the longitudinal position ordering $\xi_i < \xi_{i+1}$ of subsequent interactions. The sum (4.6) over arbitrary m-fold rescattering contributions can thus be represented by a simple exponential of the dipole cross section

$$F\left(\mathbf{u},\bar{\mathbf{y}}\right) = e^{-i\mathbf{k}_\perp\cdot(\mathbf{u}-\bar{\mathbf{y}})} \times \exp\left(-\frac{1}{2}\int_{\bar{y}_l}^{z_+} d\xi\, n(\xi)\,\sigma\left(\mathbf{u}-\bar{\mathbf{y}}\right)\right). \quad (4.11)$$

2. Rescattering for $y_l < \xi < \bar{y}_l$

The rescattering in the region $y_l < \xi < \bar{y}_l$ is described by the path integral M of (4.2). To simplify this expression, we start from its $n = 1$ first order contribution in opacity

$$M^{(n=1)}(\mathbf{r}_1,\mathbf{r}_2,\mathbf{r}_3|y_l,\bar{y}_l) = C_A\int\frac{d\boldsymbol{q}_{1\perp}}{(2\pi)^2}\,|a_0(\boldsymbol{q}_{1\perp})|^2 \times\int_{y_l}^{\bar{y}_l} d\xi_1\, n(\xi_1)\int d\mathbf{r}_1(\xi_1)\,d\mathbf{r}_2(\xi_1)\,d\mathbf{r}_3(\xi_1) \times M_0(\mathbf{r}_1,\mathbf{r}_2,\mathbf{r}_3|y_l,\xi_1)\,M_0(\mathbf{r}_1,\mathbf{r}_2,\mathbf{r}_3|\xi_1,\bar{y}_l) \times\left(e^{i\boldsymbol{q}_{1\perp}\cdot(\mathbf{r}_3(\xi_1)-\mathbf{r}_1(\xi_1))}-1\right). \quad (4.12)$$

Here, M_0 denotes the non-interacting part of M, obtained by replacing $\tilde{G}\to G_0$ in (4.2). The dipole cross section (4.7) can be identified with the $\boldsymbol{q}_{1\perp}$-integral. Equation (4.12) allows for an iteration to arbitrary order n. Writing the free Green's functions of M_0 in a path-integral representation, using $\dot{\mathbf{r}} = d\mathbf{r}/d\xi$, we find

$$M(\mathbf{r}_1,\mathbf{r}_2,\mathbf{r}_3|y_l,\bar{y}_l) = \int\mathcal{D}\mathbf{r}_1\,\mathcal{D}\mathbf{r}_2\,\mathcal{D}\mathbf{r}_3 \times\exp\left[i\frac{E}{2}\int_{y_l}^{\bar{y}_l} d\xi\left(x\,\dot{\mathbf{r}}_3^2+(1-x)\,\dot{\mathbf{r}}_2^2-\dot{\mathbf{r}}_1^2\right)\right] \times\exp\left[-\frac{1}{2}\int_{y_l}^{\bar{y}_l} d\xi n(\xi)\sigma\left(\mathbf{r}_3-\mathbf{r}_1\right)\right]. \quad (4.13)$$

3. Radiation cross section in terms of the colour dipole

The medium-dependence of the radiation cross section (4.1) is contained in the functions F and M of (4.11) and (4.13). It is parametrized in terms of the colour dipole cross section σ and the density of scattering centers $n(\xi)$. Inserting the expressions (4.11) and (4.13) for F and M into (4.1), a substantial amount of straightforward algebra allows for further simplifications. Two of the three path-integrals in (4.13) and some of the transverse integrals in (4.1) can be done analytically. We give these technical details in appendix D. The final result for the radiation cross section (3.13) depends to leading $O(x)$ on one path integral only

$$\mathcal{K}(\mathbf{r}(y_l),y_l;\mathbf{r}(\bar{y}_l),\bar{y}_l|\omega) = \int\mathcal{D}\mathbf{r}\exp\left[\int_{y_l}^{\bar{y}_l} d\xi\left(i\frac{\omega}{2}\dot{\mathbf{r}}^2-\frac{1}{2}n(\xi)\sigma\left(\mathbf{r}\right)\right)\right], \quad (4.14)$$

and takes the explicit form

$$\frac{d^3\sigma^{(in)}}{d(\ln x)\,d\mathbf{k}_\perp} = \frac{\alpha_s}{(2\pi)^2}\,\frac{1}{\omega^2}\,N_C\,C_F\,2\mathrm{Re}\int_{z_-}^{z_+} dy_l\int_{y_l}^{z_+} d\bar{y}_l \times e^{-\epsilon|y_l|-\epsilon|\bar{y}_l|}\int d\mathbf{u}\,e^{-i\mathbf{k}_\perp\cdot\mathbf{u}}\,e^{-\frac{1}{2}\int_{\bar{y}_l}^{z_+} d\xi\,n(\xi)\,\sigma(\mathbf{u})} \times\frac{\partial}{\partial\mathbf{y}}\cdot\frac{\partial}{\partial\mathbf{u}}\,\mathcal{K}(\mathbf{y}=0,y_l;\mathbf{u},\bar{y}_l|\omega)\,. \quad (4.15)$$

This is the main result of the present section. It contains all the characteristic features of the result of Zakharov [8], and the extension of Zakharov's result to finite transverse momentum [12, 13]. The dipole cross section $\sigma(\boldsymbol{\rho})$ is the leading $O(x)$ contribution of the q-$\bar{q}$-g cross section introduced by Nikolaev and Zakharov [21] and used in [8, 13]. The reason why this cross section depends on only one impact parameter $\boldsymbol{\rho}$ is evident from (3.13): in principle, rescattering contributions can compare the transverse position between the three combinations $q-q$, $q-g$ or $g-g$ in amplitude and complex conjugate amplitude. In the leading $O(x)$ approximation, however, the transverse position of the quark remains unchanged due to rescattering. Moreover, the difference between the transverse paths of the gluon in amplitude and complex conjugate amplitude which is given by the function F in (4.11), is fixed by the measured transverse momentum $\mathbf{k}_\perp$ and shows no time (i.e. ξ-) evolution. Accordingly, there is only one remaining impact parameter which measures the transverse separation of the gluon from the quark.

The result (4.15) is closely related to the QED radiation cross section, see Eq. (5.13) below. The result (4.15) differs from the expressions given by Zakharov [8, 13] by (i) including the ϵ-regularization and (ii) not subtracting from $\mathcal{K}$ in (4.15) the zeroth order term $\mathcal{K}_0$. As discussed elsewhere in detail [12], (i) is indispensable for a quantitative analysis of the radiation cross section. The subtraction of $\mathcal{K}_0$ was included in Ref. [8, 13] to cancel a potentially dangerous singularity of the path-integral $\mathcal{K}$. However, in the presence of the ϵ-regularization, this singularity does not exist and the $\mathcal{K}_0$-term vanishes. It can thus be included for technical convenience, but it is not needed.

Our derivation of (4.15) provides a new and direct proof of the equivalence of the BDMPS- and Zakharov-formalism. In fact, the non-abelian Furry approximation which allowed us to write the high-energy limit of (2.4) is a compact shorthand of all the rescattering diagrams included in the analysis of BDMPS [19]. Obtaining from this starting point the path-integral expression (4.15) proves the equivalence. It is an independent confirmation of the corresponding statements in Ref. [10], and extends these arguments explicitly to the $\mathbf{k}_\perp$-differential radiation cross section.

V. PROBABILITY CONSERVATION TO FIXED ORDER IN OPACITY

In this section, we introduce a new quantity $\sigma_{\rm cl}$, obtained by factorizing out of the radiation cross section (4.15) a momentum independent absorption factor,

$$\frac{d^3\sigma^{(in)}}{d(\ln x)\,d\mathbf{k}_\perp} = e^{-\int d\xi\, n(\xi)\, V_{\rm tot}}\, \frac{d^3\sigma_{\rm cl}}{d(\ln x)\,d\mathbf{k}_\perp}\,. \tag{5.1}$$

Here, $V_{\rm tot}$ denotes the total elastic cross section for the projectile scattering off one scattering center. In what follows, we argue that the N-th order opacity term of $\sigma_{\rm cl}$ reduces in the coherent and incoherent limiting cases to the classically expected results for bremsstrahlung associated to N-fold scattering. In the incoherent limit, it becomes the incoherent sum of N Gunion-Bertsch radiation terms

$$\lim_{L\to\infty} \frac{d^3\sigma_{\rm cl}(N)}{d(\ln x)\,d\mathbf{k}_\perp}\bigg|_{L\,n_0=\text{fixed}} \equiv \frac{\alpha_s}{\pi^2}\,N_c\,C_F\,\frac{(L\,n_0)^N}{N!} \times \left(\prod_{i=1}^N \int_{q_i}\right) \sum_{i=1}^N R\left(\mathbf{k}_\perp + \sum_{j=1}^{i-1} \boldsymbol{q}_{j\perp}, \boldsymbol{q}_{i\perp}\right)\,. \tag{5.2}$$

In the coherent limit, it reduces to a single Gunion-Bertsch radiation term for the combined momentum transfer of N single scattering centers,

$$\lim_{L\to 0} \frac{d^3\sigma_{\rm cl}(N)}{d(\ln x)\,d\mathbf{k}_\perp}\bigg|_{L\,n_0=\text{fixed}} \equiv \frac{\alpha_s}{\pi^2}\,N_c\,C_F\,\frac{(L\,n_0)^N}{N!} \times \left(\prod_{i=1}^N \int_{q_i}\right) R\left(\mathbf{k}_\perp, \sum_{i=1}^N \boldsymbol{q}_{i\perp}\right)\,. \tag{5.3}$$

In what follows, all limits $L\to 0$ and $L\to\infty$ are taken at fixed opacity $L\,n_0 =$ fixed without specifying this explicitly. The N-th order contribution of (5.1) reads

$$\frac{d^3\sigma^{(in)}(N)}{d(\ln x)\,d\mathbf{k}_\perp} = \sum_{m=0}^N (-1)^m\, w_m\, \frac{d^3\sigma_{\rm cl}(N-m)}{d(\ln x)\,d\mathbf{k}_\perp}\,, \tag{5.4}$$

where the weights w_m are the m-th order terms of the absorption factor

$$w_m = \frac{1}{m!}\left(\int d\xi\, n(\xi)\, V_{\rm tot}\right)^m\,. \tag{5.5}$$

These weights will be seen to appear as a consequence of probability conservation. In section V A, we discuss the above relations for QED. In section V B, we extend this discussion to QCD.

A. Elastic scattering and radiation in QED

In the present subsection, we take

$$V(\boldsymbol{q}_\perp) = |\bar a_0(\boldsymbol{q}_\perp)|^2\,, \tag{5.6}$$

$$V_{\rm tot} = \int \frac{d\boldsymbol{q}_\perp}{(2\pi)^2} |\bar a_0(\boldsymbol{q}_\perp)|^2\,, \tag{5.7}$$

to be the differential and total elastic scattering cross section for an electron scattering off a single electrically charged static potential. In general, we distinguish by a bar the QED quantities used in this subsection from their QCD counterparts discussed in the rest of this paper. The QED dipole cross section is defined by

$$\bar\sigma(\boldsymbol{\rho}) = 2\int \frac{d\boldsymbol{q}_\perp}{(2\pi)^2}\,|\bar a_0(\boldsymbol{q}_\perp)|^2\,\left(1-e^{-i\boldsymbol{q}_\perp\cdot\boldsymbol{\rho}}\right)\,, \tag{5.8}$$

and the Fourier transform of $\bar\sigma$ takes the form [12]

$$\bar\Sigma(\mathbf{q}_\perp) = \frac{1}{2}\int \frac{d\boldsymbol{\rho}}{(2\pi)^2}\,\bar\sigma(\boldsymbol{\rho})\,e^{i\mathbf{q}_\perp\cdot\boldsymbol{\rho}} = -V(\mathbf{q}_\perp) + V_{\rm tot}\,\delta^{(2)}(\mathbf{q}_\perp)\,. \tag{5.9}$$

Furthermore, we denote by

$$\bar R(\mathbf{k}_\perp, \mathbf{q}_\perp) = \frac{x^2\mathbf{q}_\perp^2}{\mathbf{k}_\perp^2\,(\mathbf{k}_\perp + x\mathbf{q}_\perp)^2} \tag{5.10}$$

the momentum dependence of a Bethe-Heitler radiation term associated with the incoming electron momentum $\mathbf{k}_\perp$ and the scattering momentum transfer $\mathbf{q}_\perp$. Finally, we introduce two shorthands for the average over the transverse momenta $\mathbf{q}_{i\perp}$ of the different scattering centers. Depending on whether this average involves the term $\propto V_{\rm tot}\,\delta^{(2)}(\mathbf{q}_\perp)$ in (5.12) or not, we write

$$\int_{\bar\Sigma_N} \equiv (-1)^N \prod_{i=1}^N \int d\mathbf{q}_{i\perp}\,\bar\Sigma(\mathbf{q}_{i\perp})\,, \tag{5.11}$$

$$\int_{\mathbf{q}_i} \equiv \int \frac{d\mathbf{q}_{i\perp}}{(2\pi)^2}\,|\bar a_0(\mathbf{q}_{i\perp})|^2\,. \tag{5.12}$$

The QED radiation cross section derived in [12, 13] can be obtained from (4.15) by substituting the QED dipole cross section $\bar\sigma$ of (5.8) for the QCD one, and by changing the coupling strength $\alpha_{\rm s}\,N_c\,C_F \to \alpha_{\rm em}$,

$$\frac{d^3\bar\sigma^{(in)}}{d(\ln x)\,d\mathbf{k}_\perp} = \frac{\alpha_{\rm em}}{(2\pi)^2}\,\frac{1}{\omega^2}\,2{\rm Re}\int_{z_-}^{z_+} dy_l \int_{y_l}^{z_+} d\bar y_l \times e^{-\epsilon|y_l|\,-\epsilon|\bar y_l|}\int d\mathbf{u}\, e^{-i\mathbf{k}_\perp\cdot\mathbf{u}}\, e^{-\frac{1}{2}\int_{z_-}^{y_l} d\xi\, n(\xi)\,\bar\sigma(\mathbf{u})} \times\frac{\partial}{\partial\mathbf{y}}\cdot\frac{\partial}{\partial\mathbf{u}}\,\mathcal{K}(\mathbf{y}=0,y_l;\mathbf{u},\bar y_l|\omega)\,. \tag{5.13}$$

In contrast to the QCD case (4.15), the term $\exp\left(-\frac{1}{2}\int_{z_-}^{y_l} d\xi\, n(\xi)\,\bar\sigma(\mathbf{u})\right)$ in (5.13) ranges from z_- to y_l [12] since it is the rescattering of the incoming charged projectile (and not the rescattering of the outgoing radiated particle as in QCD) which determines the QED radiation spectrum.

The following argument is based on the observation that the term $\propto V_{\rm tot}\,\delta^{(2)}(\mathbf{q}_\perp)$ in (5.9) can be factored out of (5.13) in form of the absorption factor in (5.1). The quantity $\sigma_{\rm cl}$ depends only on $V(\mathbf{q}_\perp)$. Moreover, the N-th order term of the radiation cross section (5.13) depends only on the (Fourier transform) of the dipole cross section (5.9), i.e., it is written with the averages (5.11). This suggests that $\sigma_{\rm cl}$ takes a simple form if written in terms of the averages (5.12). To make more specific statements, we now investigate the first few terms in the opacity expansion of (5.13) which were calculated in Ref. [12].

The $N=1$ term is the Bethe-Heitler radiation cross section times the opacity $L\,n_0$ of the medium,

$$\frac{d^3\bar\sigma^{(in)}(N=1)}{d(\ln x)\,d\mathbf{k}_\perp} = \frac{\alpha_{\rm em}}{\pi^2}\,(L\,n_0)\int_{\bar\Sigma_1}\bar R(\mathbf{k}_\perp,\mathbf{q}_{1\perp}) = \frac{\alpha_{\rm em}}{\pi^2}\,(L\,n_0)\int_{\mathbf{q}_1}\bar R(\mathbf{k}_\perp,\mathbf{q}_{1\perp})\,. \tag{5.14}$$

This confirms (5.4) up to first order in opacity. Since the Bethe-Heitler term vanishes for vanishing momentum transfer, the two medium averages (5.11) and (5.12) make no difference for this term. This is different for the higher order terms for which we discuss here the coherent and incoherent limits.

For two scattering centers, the radiation cross section takes the coherent limit [12]

$$\lim_{L\to 0}\frac{d^3\bar\sigma^{(in)}(N=2)}{d(\ln x)\,d\mathbf{k}_\perp} = \frac{\alpha_{\rm em}}{\pi^2}\frac{(L\,n_0)^2}{2}\int_{\bar\Sigma_2}\bar R(\mathbf{k}_\perp,\mathbf{q}_{1\perp}+\mathbf{q}_{2\perp}) = \frac{\alpha_{\rm em}}{\pi^2}\frac{(L\,n_0)^2}{2}\left(\int_{\mathbf{q}_1}\int_{\mathbf{q}_2}\bar R(\mathbf{k}_\perp,\mathbf{q}_{1\perp}+\mathbf{q}_{2\perp}) -2\,V_{\rm tot}\int_{\mathbf{q}_1}\bar R(\mathbf{k}_\perp,\mathbf{q}_{1\perp})\right)\,. \tag{5.15}$$

Here, the first line is the result obtained in Ref. [12], the second line is obtained by inserting expression (5.9) and integrating out the δ-functions of the terms $\propto V_{\rm tot}\,\delta^{(2)}(\mathbf{q}_\perp)$. In the incoherent limit, we find in the same way

$$\lim_{L\to\infty}\frac{d^3\bar\sigma^{(in)}(N=2)}{d(\ln x)\,d\mathbf{k}_\perp} = \frac{\alpha_{\rm em}}{\pi^2}\frac{(L\,n_0)^2}{2}\int_{\bar\Sigma_2}\big[\bar R(\mathbf{k}_\perp,\mathbf{q}_{1\perp}) +\bar R(\mathbf{k}_\perp+\mathbf{q}_{1\perp},\mathbf{q}_{2\perp})\big] = \frac{\alpha_{\rm em}}{\pi^2}\frac{(L\,n_0)^2}{2}\left(\int_{\mathbf{q}_1}\int_{\mathbf{q}_2}\bar R(\mathbf{k}_\perp+\mathbf{q}_{1\perp},\mathbf{q}_{2\perp}) -V_{\rm tot}\int_{\mathbf{q}_1}\bar R(\mathbf{k}_\perp,\mathbf{q}_{1\perp})\right)\,. \tag{5.16}$$

The results (5.15), (5.16) are the QED analogue of the expressions (3.47) and (3.48) obtained for the $N=2$ QCD radiation cross section. This confirms (5.4) up to second order in opacity:

$$\frac{d^3\bar\sigma^{(in)}(N=2)}{d(\ln x)\,d\mathbf{k}_\perp} = \frac{d^3\bar\sigma_{\rm cl}(N=2)}{d(\ln x)\,d\mathbf{k}_\perp} - w_1\,\frac{d^3\bar\sigma_{\rm cl}(N=1)}{d(\ln x)\,d\mathbf{k}_\perp}\,, \tag{5.17}$$

Here, the weight $w_1=(L\,n_0\,V_{\rm tot})$ contains only information on the mean free path of the projectile. It is the probability of having one additional interaction with the medium. The physical reason for the negative terms in (5.15) and (5.16) is now obvious:

An expansion of (5.13) up to second order sums over the two possibilities that the photon was produced by an interaction of the electron with either one or two scattering centers. The probability of this second interaction is a factor w_1 smaller than the probability that only one interaction occurs. Hence, to go consistently from the first ($N=1$) to the second ($N=2$) order approximation of (5.13) requires two steps: (i) the radiation contribution related to two rescatterings of finite momentum transfers has to be added [this contribution is denoted by $\sigma_{\rm cl}$]. (ii) the probability for the $N=1$-contribution has to be reduced by a factor $(1-w_1)$ [in this way, the probabilities for the $N=1$ and $N=2$-contributions add up to unity]. The second, negative term in (5.17) implements step (ii). It is this second step which leads to the negative term in the coherent limit (5.15) and which changes the sign of the second term in the incoherent limit (5.16). To sum up: the opacity expansion of (4.15) correctly readjusts the probability of the $\sigma_{\rm cl}(N=1)$ contribution if including the higher order $N=2$ in the approximation of (4.15).

Ref. [12] also provides the third order contribution to the QED radiation cross section. The limiting cases read

$$\lim_{L\to 0}\frac{d^3\bar\sigma^{(in)}(N=3)}{d(\ln x)\,d\mathbf{k}_\perp} = \frac{\alpha_{\rm em}}{\pi^2}\frac{(L\,n_0)^3}{3!}\left(\int_{\mathbf{q}_1}\int_{\mathbf{q}_2}\int_{\mathbf{q}_3}\bar R(\mathbf{k}_\perp,\mathbf{q}_{1\perp}+\mathbf{q}_{2\perp}+\mathbf{q}_{3\perp}) -3\,V_{\rm tot}\int_{\mathbf{q}_1}\int_{\mathbf{q}_2}\bar R(\mathbf{k}_\perp,\mathbf{q}_{1\perp}+\mathbf{q}_{2\perp})\right.$$

$$+3\,V_{\rm tot}^2 \int_{\mathbf{q}_1} \bar{R}(\mathbf{k}_\perp, \mathbf{q}_{1\perp})\Big)\,, \tag{5.18}$$

$$\lim_{L\to\infty} \frac{d^3\bar{\sigma}^{(in)}(N=3)}{d(\ln x)\,d\mathbf{k}_\perp}\bigg|_{L\,n_0=\text{fixed}} = \frac{\alpha_s}{\pi^2}\,N_c\,C_F\,C_A^2\,\frac{(Ln_0)^3}{3!}$$
$$\times \int_{q_1}\int_{q_2}\int_{q_3} \big[\bar{R}(\mathbf{k}_\perp + \boldsymbol{q}_{1\perp} + \boldsymbol{q}_{2\perp}, \boldsymbol{q}_{3\perp})$$
$$-2\,\bar{R}(\mathbf{k}_\perp + \boldsymbol{q}_{1\perp}, \boldsymbol{q}_{2\perp}) + \bar{R}(\mathbf{k}_\perp, \boldsymbol{q}_{1\perp})\big]\,. \tag{5.19}$$

The relative signs and weights of different Bethe-Heitler terms confirm (5.1) to third order

$$\frac{d^3\bar{\sigma}^{(in)}(N=3)}{d(\ln x)\,d\mathbf{k}_\perp} = \frac{d^3\bar{\sigma}_{\rm cl}(N=3)}{d(\ln x)\,d\mathbf{k}_\perp} - w_1\,\frac{d^3\bar{\sigma}_{\rm cl}(N=2)}{d(\ln x)\,d\mathbf{k}_\perp}$$
$$+w_2\frac{d^3\bar{\sigma}_{\rm cl}(N=1)}{d(\ln x)\,d\mathbf{k}_\perp}\,. \tag{5.20}$$

We note that summed over arbitrary orders of opacity, the factor $\sum_{j=0}^{\infty}(-1)^j\,w_j$ in (5.4) amounts to a momentum-independent normalization. The angular distribution of gluon radiation, calculated directly from the all-order expression (5.1) is not modified by this normalization factor. In an expansion in opacity, however, the weights w_i do not factorize from the momentum dependence. The correct angular distribution for radiation off a target of N scattering centers is given by the sum over the opacity contributions up to N-th order. In this way, the results of the BDMPS/Zakharov-formalism can be compared directly to results for a finite number of scattering centers.

B. Elastic scattering and medium-induced radiation in QCD

The above arguments confirm the expressions (5.1)-(5.5) for QED, and they apply to the QCD radiation spectrum, too. This follows from the fact that the QED and QCD radiation spectrum are related by simple substitutions which do not affect the form of (4.15). In QED, however, the only total elastic scattering cross section $V_{\rm tot}$ associated to the projectile is that of the electron. In contrast, both quark and gluon are charged in QCD and have a finite elastic scattering cross section. What is additionally needed to justify (5.1)-(5.5) in QCD is an argument why the total elastic scattering cross section $V_{\rm tot}$ in (5.1)-(5.5) should be that of the gluon,

$$V_{\rm tot} = C_A \int \frac{d\boldsymbol{q}_\perp}{(2\pi)^2}|a_0(\boldsymbol{q}_\perp)|^2\,, \tag{5.21}$$

rather than that of the quark or a combination of both.

The motivation for (5.21) comes from the observation of section III A that the i-th scattering center always contributes with a factor C_A to the radiation cross section, i.e., the q-g-projectile scatters effectively with the coupling strength of a gluon. This is a consequence of the leading $O(x)$ approximation in which, as observed by BDMPS, only the rescattering of the gluon matters. Beyond the leading $O(x)$ approximation, more complicated combinations of elastic quark and gluon cross sections may be needed, but this is the regime in which colour triviality breaks down and our formalism does not apply.

In analogy to the QED case, we can argue on the basis of (5.1) and (5.21) that the N-th order opacity term of the QCD radiation cross section (4.15) is a convolution of the N-fold scattering contribution and a readjustment of the probabilities that less than N rescatterings occur. This explains especially the structure of the $N=2$ QCD contributions calculated in section III D. More details about the opacity expansion for QCD are given in the next section and in Appendix E.

VI. IN-MEDIUM PRODUCTION: HARD VERSUS MEDIUM-INDUCED RADIATION

The initial state boundary condition in the above calculations is that of a quark approaching an asymptotic plane wave (2.9) at far backward positions. In relativistic heavy ion collisions, however, the hard (off-shell) parton is produced inside the collision region and its propagation inside the medium has to be followed from a fixed finite time onwards. In what follows, we discuss the corresponding gluon radiation cross section $\sigma^{(nas)}$ for a *nascent* quark, in contrast to the case for a free *in*coming quark which was discussed in sections II-V.

The radiation cross section $\sigma^{(nas)}$ for nascent quarks is obtained by making two simple modifications to our derivation in sections II-IV:

(i) At the beginning of our derivation in section II, one has to replace the incoming plane wave $F(\mathbf{x}, p_1)$ by a production amplitude $J(p_1)$ which specifies the probability that at some point $(z_0, \mathbf{0}_\perp, z_0)$ in the collision region a hard parton of momentum p_1 is produced. We follow Gyulassy, Levai and Vitev [17] in factorizing the production probability $|J(p_1)|^2$ out of the radiation cross section. This is an assumption on the weak momentum dependence of this source which is also implicitly present in other discussions of radiative energy loss from partons produced in medium [8]. Since our starting point (2.18) is written for $\mathbf{p}_{1\perp}=0$, i.e., $F(\mathbf{x}, p_1)=1$, this amounts to multiplying (2.18) by a factor $|J(p_1)|^2$. To simplify notation, we drop this factor in what follows: in comparing to experiment, the radiation cross section $\sigma^{(nas)}$ given below has to be weighted with the production probability of the hard parton.

(ii) The parton produced at $(z_0, \mathbf{0}_\perp, z_0)$ propagates in the positive z-direction. Accordingly, the gluon emission vertices in the amplitude and complex conjugate amplitude

are constrained to longitudinal positions y_l, $\bar{y}_l > z_0$. This changes the boundaries of the corresponding integrals in (2.18) and survives all intermediate steps.

With these two changes in (2.18), and choosing $z_0 = 0$, the medium-induced gluon radiation cross section off a nascent quark becomes

$$\begin{aligned}\frac{d^3\sigma^{(nas)}}{d(\ln x)\,d\mathbf{k}_\perp} &= \frac{\alpha_s}{(2\pi)^2}\,\frac{1}{\omega^2}\,N_C\,C_F \\ &\times 2\mathrm{Re}\int_0^{z_+} dy_l \int_{y_l}^{z_+} d\bar{y}_l\, e^{-\epsilon|y_l|\,-\epsilon|\bar{y}_l|} \\ &\times \int d\mathbf{u}\, e^{-i\mathbf{k}_\perp\cdot\mathbf{u}}\, e^{-\frac{1}{2}\int_{\bar{y}_l}^{z_+} d\xi\, n(\xi)\,\sigma(\mathbf{u})} \\ &\times \frac{\partial}{\partial\mathbf{y}}\cdot\frac{\partial}{\partial\mathbf{u}}\,\mathcal{K}(\mathbf{y}=0, y_l; \mathbf{u}, \bar{y}_l|\omega)\,. \end{aligned} \tag{6.1}$$

This differs from the corresponding result of Zakharov [13] by the regularization prescription only.

In what follows, we shall analyze (6.1) in the opacity expansion. To this end, we expand the path-integral $\mathcal{K}$

$$\begin{aligned}&\mathcal{K}(\mathbf{r}, y_l; \bar{\mathbf{r}}, \bar{y}_l) = \mathcal{K}_0(\mathbf{r}, y_l; \bar{\mathbf{r}}, \bar{y}_l) \\ &-\int_z^{z'} d\xi\, n(\xi) \int d\boldsymbol{\rho}\, \mathcal{K}_0(\mathbf{r}, y_l; \boldsymbol{\rho}, \xi)\,\frac{1}{2}\,\sigma(\boldsymbol{\rho})\,\mathcal{K}_0(\boldsymbol{\rho}, \xi; \bar{\mathbf{r}}, \bar{y}_l) \\ &+\int_z^{z'} d\xi_1\, n(\xi_1) \int_{\xi_1}^{z'} d\xi_2\, n(\xi_2) \int d\boldsymbol{\rho}_1\, d\boldsymbol{\rho}_2\, \mathcal{K}_0(\mathbf{r}, y_l; \boldsymbol{\rho}_1, \xi_1) \\ &\times\frac{1}{2}\,\sigma(\boldsymbol{\rho}_1)\,\mathcal{K}(\boldsymbol{\rho}_1, \xi_1; \boldsymbol{\rho}_2, \xi_2)\,\frac{1}{2}\,\sigma(\boldsymbol{\rho}_2)\,\mathcal{K}_0(\boldsymbol{\rho}_2, \xi_2; \bar{\mathbf{r}}, \bar{y}_l)\,. \end{aligned} \tag{6.2}$$

Here, we have suppressed the explicit ω-dependence in $\mathcal{K}$. The corresponding free Green's function $\mathcal{K}_0$ reads

$$\mathcal{K}_0(\mathbf{r}, y_l; \bar{\mathbf{r}}, \bar{y}_l) = \frac{\omega}{2\pi\, i\,(\bar{y}_l - y_l)} \exp\left\{\frac{i\omega\,(\bar{\mathbf{r}}-\mathbf{r})^2}{2\,(\bar{y}_l - y_l)}\right\}. \tag{6.3}$$

The technical steps involved in the opacity expansion are described in detail in Ref. [12]. We present our result for the N-th order opacity contribution to (6.1) in the form

$$\begin{aligned}\frac{d^3\sigma^{(*)}(N)}{d(\ln x)\,d\mathbf{k}_\perp} &= \frac{\alpha_s}{(2\pi)^2}\,\frac{1}{\omega^2}\,N_C\,C_F\,2\int_{\Sigma_N}\sum_{j=0}^{N} \\ &\times\left[\mathcal{Z}^{(*)}_{N,j+1}\left(\mathbf{k}_\perp + \sum_{i=1}^{N}\mathbf{q}_{i\perp}\right)\cdot\left(\mathbf{k}_\perp + \sum_{i=1}^{N-j}\mathbf{q}_{i\perp}\right)\right], \end{aligned} \tag{6.4}$$

where the integration is defined by (5.11) and the factors $\mathcal{Z}^{(*)}_{N,j}$ are tabulated in Appendix E. The superscript ($* = in$ or $* = nas$) indicates that the result differs for the radiation cross sections (4.15) and (6.1) by the specific form of the factor $\mathcal{Z}^{(*)}_{N,j}$ only. We have checked the form of (6.4) for $N \le 3$ by explicit calculation, but we expect that it holds for arbitrary N. Especially, it is obvious that the N-th order term contains exactly $(N+1)$ different terms: the j-th term in (6.4) corresponds to the $(N-j)$-th order expansion in $\mathcal{K}$ and the j-th order expansion of the exponential $\exp\left[-\frac{1}{2}\int d\xi\, n(\xi)\,\sigma(\mathbf{u})\right]$. Moreover, each integrand in (6.4) has to depend on all N transverse momenta, since the integration (5.11) leads to a vanishing contribution otherwise.

The N-th order opacity expansion of (6.1) involves only $(N+1)$ different terms. This is a significant simplification in comparison to brute force calculations [17] which require already for $N = 2$ the calculation of 7^2 direct plus 2×96 contact terms [23]. In what follows, we discuss the physics contained in this opacity expansion by studying the coherent and incoherent limits of (6.4).

A. Hard radiation and its $N = 1$ modification

For the gluon radiation spectrum (4.15) of a free incoming quark, the zeroth order in opacity vanishes. A free incoming particle does not radiate without interaction. A nascent parton, however, does radiate without further interaction. To zeroth order in $L\,n_0$, we find

$$\frac{d^3\sigma^{(nas)}(N=0)}{d(\ln x)\,d\mathbf{k}_\perp} = \frac{\alpha_s}{\pi^2}\,N_C\,C_F\,\frac{1}{\mathbf{k}_\perp^2}\,. \tag{6.5}$$

This is the characteristic gluon radiation spectrum

$$H(\mathbf{k}_\perp) = \frac{1}{\mathbf{k}_\perp^2}\,, \tag{6.6}$$

associated to the production of a hard parton. In energy loss calculations which integrate over ω, the above radiation cross section (6.5) as well as its medium-dependent form should be multiplied with the quark-gluon splitting function $\frac{x}{2}\frac{1+(1-x)^2}{x}$ which equals one only in the $O(x)$ approximation [14]. Equation (6.5) is the QCD analogue of the QED radiation accompanying β-decay. To determine the energy loss of hard partons in relativistic heavy ion collisions, we are interested in the medium-dependent changes of the radiation cross section (6.5). To first order in opacity, we find from Appendix E

$$\begin{aligned}\frac{d^3\sigma^{(nas)}(N=1)}{d(\ln x)\,d\mathbf{k}_\perp} &= \frac{\alpha_s}{\pi^2}\,\frac{N_C\,C_F}{2\,\omega^2}\int_{\Sigma_1}\frac{-\mathbf{k}_\perp\cdot\mathbf{q}_\perp}{Q\,Q_1} \\ &\times n_0\,\frac{LQ_1 - \sin(LQ_1)}{Q_1}\,. \end{aligned} \tag{6.7}$$

To understand the physical meaning of this expression it helps to rewrite the coherent and incoherent limiting cases in terms of the hard and Gunion-Bertsch term:

$$\lim_{L\to 0}\frac{d^3\sigma^{(nas)}(N=1)}{d(\ln x)\,d\mathbf{k}_\perp} = 0\,, \tag{6.8}$$

$$\begin{aligned}\lim_{L\to\infty}\frac{d^3\sigma^{(nas)}(N=1)}{d(\ln x)\,d\mathbf{k}_\perp} &= \frac{\alpha_s}{\pi^2}\,N_C\,C_F\,(n_0\,L) \\ &\times\int_{\Sigma_1}\left[H(\mathbf{k}_\perp + \mathbf{q}_{1\perp}) + R(\mathbf{k}_\perp, \mathbf{q}_{1\perp})\right]. \end{aligned} \tag{6.9}$$

In the incoherent $L \to \infty$ limit, the radiation cross section (6.1) expanded up to first order in opacity, takes the form

$$\lim_{L\to\infty} \sum_{m=0}^{N=1} \frac{d^3\sigma^{(nas)}(m)}{d(\ln x)\, d\mathbf{k}_\perp} = \frac{\alpha_s}{\pi^2}\, N_C\, C_F \times \left[(1-w_1) H(\mathbf{k}_\perp) + n_0\, L \int_{\mathbf{q}_1} H(\mathbf{k}_\perp + \mathbf{q}_{1\perp}) + n_0\, L \int_{\mathbf{q}_1} R(\mathbf{k}_\perp, \mathbf{q}_{1\perp}) \right] . \quad (6.10)$$

The three terms on the r.h.s. of (6.10) have a simple physical meaning: the first is the hard, medium-independent radiation (6.6) reduced by the probability $w_1 = n_0\, L\, V_{\rm tot}$ that one interaction of the projectile occurs in the medium. The second term describes the hard radiation component which rescatters once in the medium. The third term is the medium-induced Gunion-Bertsch contribution associated with the rescattering. In general, the L-dependence of (6.7) reflects the interference pattern between the different contributions and can be quite complicated. For the case $N = 1$, we have seen that this interference pattern interpolates between simple and physically intuitive limiting cases.

B. Coherent and Incoherent Limits for $N = 2$ and $N = 3$

The general L-dependent expressions for the second and third orders in the opacity expansion of (6.1) can easily be written down by using (6.4) and the corresponding results tabulated in Appendix E. In the present section, we focus entirely on the coherent and incoherent limiting cases. For $N = 2$, they read

$$\lim_{L\to 0} \frac{d^3\sigma^{(nas)}(N=2)}{d(\ln x)\, d\mathbf{k}_\perp} = 0\,, \quad (6.11)$$

$$\lim_{L\to\infty} \frac{d^3\sigma^{(nas)}(N=2)}{d(\ln x)\, d\mathbf{k}_\perp} = \frac{\alpha_s}{\pi^2}\, N_C\, C_F\, \frac{(n_0\, L)^2}{2} \times \int_{\Sigma_2} \left[H(\mathbf{k}_\perp + \mathbf{q}_{1\perp} + \mathbf{q}_{2\perp}) + R(\mathbf{k}_\perp + \mathbf{q}_{1\perp}, \mathbf{q}_{2\perp}) \right] . \quad (6.12)$$

Adding this second order contribution to (6.10), a simple systematic starts to emerge:

$$\lim_{L\to\infty} \sum_{m=0}^{N=2} \frac{d^3\sigma^{(nas)}(m)}{d(\ln x)\, d\mathbf{k}_\perp} = \frac{\alpha_s}{\pi^2}\, N_C\, C_F \times \left[(1 - w_1 + w_2)\, H(\mathbf{k}_\perp) + (1-w_1)\, n_0\, L \int_{\mathbf{q}_1} H(\mathbf{k}_\perp + \mathbf{q}_{1\perp}) + \frac{(n_0\, L)^2}{2} \int_{\mathbf{q}_1} \int_{\mathbf{q}_2} H(\mathbf{k}_\perp + \mathbf{q}_{1\perp} + \mathbf{q}_{2\perp}) \right] + \lim_{L\to\infty} \left[\frac{d^3\sigma_{\rm cl}(2)}{d(\ln x)\, d\mathbf{k}_\perp} + (1-w_1)\, \frac{d^3\sigma_{\rm cl}(1)}{d(\ln x)\, d\mathbf{k}_\perp} \right] . \quad (6.13)$$

Both the m-fold rescattered hard term and the Gunion Bertsch contribution for m-fold rescattering are weighted with the expansion of the absorption factor up to order $(N - m)$. For $N = 3$, we find from the results in Appendix E

$$\lim_{L\to 0} \frac{d^3\sigma^{(nas)}(N=3)}{d(\ln x)\, d\mathbf{k}_\perp} = 0\,, \quad (6.14)$$

$$\lim_{L\to\infty} \frac{d^3\sigma^{(nas)}(N=3)}{d(\ln x)\, d\mathbf{k}_\perp} = \frac{\alpha_s}{\pi^2}\, N_C\, C_F\, \frac{(n_0\, L)^3}{3!} \times \int_{\Sigma_3} \left[H(\mathbf{k}_\perp + \mathbf{q}_{1\perp} + \mathbf{q}_{2\perp} + \mathbf{q}_{3\perp}) + R(\mathbf{k}_\perp + \mathbf{q}_{1\perp} + \mathbf{q}_{2\perp}, \mathbf{q}_{3\perp}) \right] . \quad (6.15)$$

Adding this contribution to (6.13) confirms the indicated systematics. Rather than spelling out the result, we extrapolate in the following section our analytical findings to arbitrary N.

C. Extrapolation of limiting cases to arbitrary N

The results of our explicit calculations up to third order, combined with the physical arguments given above, suggest results valid to arbitrary orders N. For the case of a free incoming quark, these results are given in equations (5.2) - (5.4). For the case of an in-medium produced quark, we write them in terms of the shorthand

$$H^{(m)}(\mathbf{k}_\perp) \equiv \frac{\alpha_{\rm s}}{\pi^2} N_c\, C_F\, \frac{(n_0\, L)^m}{m!} \left(\prod_{i=1}^{m} \int_{\mathbf{q}_i} \right) \times H\left(\mathbf{k}_\perp + \sum_{i=1}^{m} \mathbf{q}_{i\perp} \right) . \quad (6.16)$$

This describes the hard radiation component which rescatters on m well-separated scattering centers. For the incoherent limit of (6.1), expanded up to N-th order, we obtain by extrapolating the systematics observed up to $N = 3$:

$$\lim_{L\to\infty} \sum_{m=0}^{N} \frac{d^3\sigma^{(nas)}(m)}{d(\ln x)\, d\mathbf{k}_\perp} = \sum_{m=0}^{N} (-1)^{N-m}\, w_{N-m}\, H^{(m)}(\mathbf{k}_\perp) + \sum_{m=0}^{N} (-1)^{N-m}\, w_{N-m} \lim_{L\to\infty} \frac{d^3\sigma_{\rm cl}(m)}{d(\ln x)\, d\mathbf{k}_\perp} . \quad (6.17)$$

In the coherent limit, we infer from (6.11) and (6.14):

$$\lim_{L\to 0} \sum_{m=0}^{N} \frac{d^3\sigma^{(nas)}(m)}{d(\ln x)\, d\mathbf{k}_\perp} = \frac{\alpha_s}{\pi^2}\, N_C\, C_F\, \frac{1}{\mathbf{k}_\perp^2} . \quad (6.18)$$

In this coherent limit, there is no medium modification to the hard radiation (6.5), irrespective of the opacity of the target: locating the medium at (and only at) the creation

point of the parton, the projectile looses the possibility of interacting with the medium.

What matters physically is, how medium-effects switch on with increasing thickness L of the medium. This L-dependence will interpolate smoothly between the totally coherent and totally incoherent limits discussed here.

VII. CONCLUSION

Colour triviality is an important tool in the study of the nuclear dependence of hard QCD processes. For colour trivial observables, the N-fold gluon exchange with the nuclear environment reduces to the N-th power of a colour Casimir operator. This renders the calculational problem abelian.

In the present work, we have given a simple diagrammatic proof of the colour triviality for the N-th order opacity contribution to the $\mathbf{k}_\perp$-differential gluon radiation cross section off a hard quark. The diagrammatic identities developped to this end are a direct consequence of the non-abelian Furry approximation for hard partons in a nuclear environment. Summing up the contributions to the radiation cross sections to all orders in opacity, we have derived Zakharov's path-integral formalism and we have given a new proof of its equivalence to the BDMPS-formalism.

For practical applications, it is important that our approach gives an easy access to the low opacity expansion of the radiation cross sections (4.15) and (6.1). The N-th order term involves only $(N+1)$ terms which are relatively easy to calculate. In contrast to previous brute force calculations [17] which have to deal with an exponentially increasing number of terms, our approach is thus well-suited for the calculation of a realistic number of scattering centers. This is illustrated by the simple form of our explicit results up to third order in opacity.

As discussed in section V, the information contained in the N-th order opacity term to the gluon radiation cross section is a convolution of (i) the radiation associated to the rescattering off N scattering centers and (ii) a readjustment of the probabilities that rescattering occurs with $m < N$ scattering centers only. We have shown how to disentangle this information by factorizing in (5.1) the radiation cross section into two terms. In this way, at least the coherent and incoherent limits of the involved L-dependent interference pattern became accessible analytically to arbitrary order.

Most important for applications to relativistic heavy ion collisions at RHIC and LHC, we have extended these results in section VI to the gluon radiation off quarks produced in the medium. The corresponding radiation cross section (6.1) gives access to the interference pattern between the hard radiation (associated to the production of the hard parton) and the medium-induced radiation. Its coherent limit shows no medium dependence. The incoherent limit confirms the classical picture of an incoherent sum of rescattering contributions of the hard radiation and Gunion-Bertsch radiation terms. The dependence of gluon radiation on the thickness L of the medium is expected to interpolate smoothly between these analytically accessible limiting cases. The detailed study of this L-dependence awaits further work, not only in the opacity expansion discussed here, but also in the dipole approximation discussed previously [12].

ACKNOWLEDGMENTS

I thank S. Catani and Y. Dokshitzer for helpful discussions about section V.
Note added in proof: M. Gyulassy, P. Levai and I. Vitev informed me of an opacity expansion derived independently in [23].

APPENDIX A: NON-ABELIAN FURRY APPROXIMATION FOR RESCATTERING GLUONS

In this appendix, we simplify the gluon rescattering contribution (2.7). We consider on-shell gluons $k_\mu = (\omega, \mathbf{k}_\perp, k_l)$ with a physical transverse polarization

$$\epsilon_\mu(k) = (\epsilon_0, \boldsymbol{\epsilon}_\perp, -\epsilon_0)\,, \qquad \epsilon_0 = \frac{\boldsymbol{\epsilon}_\perp \cdot \mathbf{k}_\perp}{\omega + k_l}\,. \tag{A1}$$

To leading order in energy, the contraction of this polarization vector with the momentum dependent part of the three-gluon vertices occuring in (2.7) takes the form

$$\begin{aligned} &V_{\mu_{i-1}0\mu_i}(k_{i-1}, k_i - k_{i-1}, k_i)\,\epsilon^{\mu_i}(k) \\ &\quad = -2\,\omega\,\epsilon^{\mu_{i-1}}(k) + O(\omega^0)\,. \end{aligned} \tag{A2}$$

This allows to rewrite (2.7)

$$\begin{aligned} I^{\mu_1\,(L)}(\mathbf{y}, k) = \epsilon^{\mu_1}(k)\mathcal{P}\,\Bigg(\prod_{i=1}^{L}\int \frac{d^3\mathbf{k}_i}{(2\pi)^3}\,d^3\mathbf{x}_i \\ \times[-i\,A_0^{(g)}(\mathbf{x}_i)]\frac{-i\,(-2\,\omega)}{k_i^2 + i\,\epsilon} \\ \times\; e^{i\,\mathbf{k}_i\cdot(\mathbf{x}_i - \mathbf{x}_{i-1})}\Bigg)\; e^{-i\,\mathbf{k}\cdot\mathbf{x}_L}\,, \end{aligned} \tag{A3}$$

where we have rearranged the phases, using $\mathbf{x}_0 = \mathbf{y}$. The longitudinal momentum integrals can be done by contour integration

$$\begin{aligned} &\int \frac{dk_{i,l}}{(2\pi)}\,\frac{i}{k_i^2 + i\,\epsilon}\,e^{i\,k_{i,l}\,(x_{i,l} - x_{i-1,l})} \\ &\qquad = \frac{1}{2\,k_{i,l}}\Theta(x_{i,l} - x_{i-1,l})\,e^{i\,k_{i,l}\,(x_{i,l} - x_{i-1,l})}\,. \end{aligned} \tag{A4}$$

On the r.h.s. of this equation, $k_{i,l}$ is determined by the pole value to order $O(1/\omega)$, $k_{i,l} = \omega - \frac{k_i^2}{2\,\omega}$. Keeping in

(a.3) the norm to leading order in $1/\omega$ but the phase to next to leading order, we write

$$I^{\mu_1\,(L)}(\mathbf{y},k) = \epsilon^{\mu_1}\, e^{-\,i\,\omega\,y_l}\mathcal{P}\,\left(\prod_{i=1}^{L}\int d^3\mathbf{x}_i\,\Theta(x_{i,l}-x_{i-1,l})\right.$$
$$\left.\times\, G_0(\mathbf{x}_{i-1},\mathbf{x}_i|\omega)\,[-i\,A_0^{(g)}(\mathbf{x}_i)]\right)$$
$$\times e^{-i\,\mathbf{k}_\perp\cdot\mathbf{x}_{L,\perp}+i\frac{\mathbf{k}_\perp^2}{2\,\omega}x_{L,l}}\,, \qquad \text{(A5)}$$

where the transverse momentum integrals are identified with the free Green's functions

$$G_0(\mathbf{x}_{i-1};\mathbf{x}_i|\omega) = \int\frac{d^2\mathbf{k}_{i,\perp}}{(2\pi)^2}\,e^{i\,\mathbf{k}_{i,\perp}\cdot(\mathbf{x}_{i,\perp}-\mathbf{x}_{i-1,\perp})}$$
$$\times e^{-i\frac{k_{i,\perp}^2}{2\,\omega}(x_{i,l}-x_{i-1,l})}\,. \qquad \text{(A6)}$$

To rewrite the path-ordered product in (A5), we introduce the shorthand

$$G^{(L)}(\mathbf{y}_\perp,y_l;\mathbf{x}_\perp,x_l|\omega) =$$
$$\mathcal{P}\,\left(\prod_{i=1}^{L}\int d^3\mathbf{x}_i\,\Theta(x_{1,l}-x_{i-1,l})\right)\,G_0(\mathbf{y}_\perp,y_l;\mathbf{x}_{1,\perp},x_{1,l}|p)$$
$$\times\left(\prod_{i=1}^{L}[-i\,A_0(\mathbf{x}_i)]\,G_0(\mathbf{x}_{i,\perp},x_{i,l};\mathbf{x}_{i+1,\perp},x_{i+1,l}|p)\right)\,, \qquad \text{(A7)}$$

where $\mathbf{x}_{L+1}=\mathbf{x}$. This allows us to write

$$I^{\mu_1\,(L)}(\mathbf{y},k) = \epsilon^{\mu_1}\,e^{-\,i\,\omega\,y_l}$$
$$\times\int d\mathbf{x}_\perp G^{(L)}(\mathbf{y};\mathbf{x}|\omega)\,F(\mathbf{x},\mathbf{k})\,. \qquad \text{(A8)}$$

APPENDIX B: SIMPLIFYING THE INTERACTION VERTEX

Here, we discuss details of how to simplify the interaction vertex (2.16) in the leading $O(x)$ approximation. The $\mathbf{y}$-derivatives in the differential operators $\hat{D}_1$ and $\hat{D}_2$ are conjugate to the transverse momenta $p_{11}^\perp$ and $p_{21}^\perp$ of the quark entering and leaving the radiation vertex, see Fig. 1 for notation. As a consequence, the interaction vertex (2.15) takes a particularly simple form in a frame in which $p_{11}^\perp = p_{21}^\perp$. Depending on the spin of the ingoing ($\lambda_q=\pm\frac{1}{2}$) and outgoing ($\lambda_{q'}=\pm\frac{1}{2}$) quark and the gluon helicity ($\lambda_g=\pm1$), it reads in this frame (see Refs. [11, 12] for a derivation)

$$\hat{\Gamma}_y\big(\lambda_q=\lambda_{q'},\lambda_g\big) = -i\,\lambda_g\,\left[\lambda_g\,(2-x)+2\,\lambda_q\,x\right]$$
$$\times\left(\frac{\partial}{\partial y_1}-i\,\lambda_g\,\frac{\partial}{\partial y_2}\right)\,, \qquad \text{(B1)}$$

$$\widehat{\Gamma}_r\big(\lambda_q=-\lambda_{q'},\lambda_g\big) = 2\,m_q\,x\,\lambda_g\,\delta_{\lambda_g\,,2\lambda_q}\,, \qquad \text{(B2)}$$

where the differential operators in (B1) act on the two different transverse components $\mathbf{y}=(y_1,y_2)$ of the Green's function for the outgoing quark. The important property of this representation of the spinor structure is that the spin- and helicity-averaged combination $\hat{\Gamma}_{\mathbf{y}}\,\hat{\Gamma}^\dagger_{\mathbf{y}'}$ takes the simple form

$$\hat{\Gamma}_{\mathbf{y}}\,\hat{\Gamma}^\dagger_{\mathbf{y}'} = g_{nf}\frac{\partial}{\partial\mathbf{y}_*}\cdot\frac{\partial}{\partial\mathbf{y}'_*}+g_{sf}\,, \qquad \text{(B3)}$$

where the prefactors for the spin-flip g_{sf} and non-flip g_{nf} term read

$$g_{nf} = [4-4x+2x^2]\,, \qquad g_{sf} = 2\,m_q^2\,x^2\,. \qquad \text{(B4)}$$

For the case of photon emission, one can choose to redefine the longitudinal z-axis to be parallel to the emitted photon $\mathbf{k}$ [11, 12]. This ensures $p_{11}^\perp = p_{21}^\perp$ and allows to eliminate all spinor dependence from the radiation probability with the help of (B3) and $y_*=y$. For the gluon radiation amplitude, this trick cannot be used. The reason is that due to the rescattering of the gluon, the direction $\mathbf{k}$ of the final state gluon is not aligned to the direction $\mathbf{k}_1$ with which the gluon leaves the radiation vertex. To use the simple expression (B3) nevertheless, we introduce the derivative $-i\partial/\partial\mathbf{y}_g$, where the subscript denotes that this partial derivative is acting on the $\mathbf{y}$-dependence of the gluon Green's function $G_{(g)}$. $-i\partial/\partial\mathbf{y}_g$ is the conjugate of the direction $\mathbf{k}_{1\perp}$. In the frame parallel to $\mathbf{k}_1$, the conjugate of the momentum $p_{21}^\perp$ thus takes the form

$$\frac{\partial}{\partial\mathbf{y}}\longrightarrow\frac{\partial}{\partial\mathbf{y}_*}=\frac{\partial}{\partial\mathbf{y}}-\frac{1-x}{x}\frac{\partial}{\partial\mathbf{y}_g}\,. \qquad \text{(B5)}$$

With this replacement, the vertex functions in (B1) and (B3) can be used for the discussion of the gluon radiation spectrum in a frame in which the incoming quark momentum $\mathbf{p}_1$ defines the longitudinal direction.

In the leading $O(x)$ approximation, only the partial derivative w.r.t. $\mathbf{y}_g$ survives in (B5), the spin-flip contribution can be neglected, and the spin- and helicity averaged combination (B3) takes in momentum space the simple form (2.25).

APPENDIX C: CANCELATION OF A CLASS OF CONTACT TERMS

To arrive at the expression (3.13) for the gluon radiation cross section in the presence of N scattering centers, we have included arbitrary combinations of real and contact terms to fixed order in opacity. However, contributions to the radiation cross section have to involve at least one (real or contact) interaction in both the amplitude and complex amplitude. The reason for that is that due to energy-momentum conservation, an amplitude which is touched neither by real nor by contact terms cannot

contribute to a final state. According to this counting, diagrams which have N contact terms in one amplitude should not be included in the calculation of the $O(N)$ contribution. Here, we show that their inclusion in the derivation of (3.13) is allowed, since this set of diagrams adds up to zero at arbitrary order in opacity.

For our proof, we consider the set of $O(N)$ diagrams with N contact terms in the amplitude, and m of these contact terms occuring at longitudinal positions $> y_l$. These contributions have the form

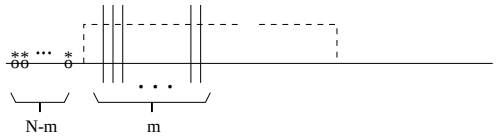

(C1)

where each thin vertical line denotes a contact term linking either twice to the quark line or twice to the gluon line or once to the quark and once to the gluon line. In what follows, we consider the subset of these diagrams which contributes to an arbitrary but fixed interaction vertex $\Gamma_{(i)}$. The longitudinal phase factor Φ associated with this set of diagrams takes the form

$$\Phi(y_l,\bar{y}_l) = \varphi(y_l)\, e^{-i\,Q\,\bar{y}_l}\,. \tag{C2}$$

The reason for this factorization of the $\bar{y}_l$-dependence is that the longitudinal positions ξ_i, $i \in [1,N]$, of the N scattering centers (which are integration variables in the calculation of Φ) do not have $\bar{y}_l$ as integration boundary. As a consequence, the only possible $\bar{y}_l$-dependence of Φ comes from the phase in the conjugate interaction free amplitude where the gluon has transverse energy Q.

For each class of diagrams (C1), we find the corresponding class of diagrams which has N contact terms on the opposite side of the cut

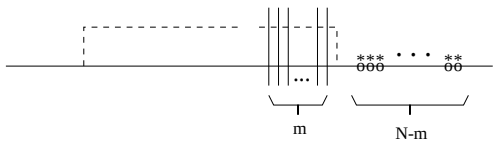

(C3)

For the class of diagrams to fixed $\Gamma_{(i)}$, the phase corresponding to (C3) reads

$$\Phi^*(\bar{y}_l,y_l) = \varphi^*(\bar{y}_l)\, e^{i\,Q\,y_l}\,. \tag{C4}$$

It is related to (C2) by complex conjugation and interchange $\bar{y}_l \leftrightarrow y_l$. The combined $\mathcal{Z}$-factor for the sum of both phases (C2) and (C4) reads according to (3.19)

$$\begin{aligned}\mathcal{Z}_{\rm comb} = 2{\rm Re}\int_{z_-}^{z_+} dy_l \int_{y_l}^{z_+} d\bar{y}_l\, e^{-\epsilon|\bar{y}_l|-\epsilon|y_l|} \\ \times\left(\Phi(y_l,\bar{y}_l)+\Phi(\bar{y}_l,y_l)\right)\,.\end{aligned} \tag{C5}$$

The second term in (C5) can be rewritten in the form

$$\begin{aligned}&\int_{z_-}^{z_+} dy_l \int_{z_-}^{z_+} d\bar{y}_l\,\Theta\left(y_l-\bar{y}_l\right)\,\Phi(\bar{y}_l,y_l) \\ &= \int_{z_-}^{z_+} dy_l \int_{z_-}^{z_+} d\bar{y}_l\,\Theta\left(\bar{y}_l-y_l\right)\,\Phi(y_l,\bar{y}_l)\,.\end{aligned} \tag{C6}$$

This allows to write for (C5)

$$\begin{aligned}\mathcal{Z}_{\rm comb} = 2{\rm Re}\int_{z_-}^{z_+} dy_l \int_{z_-}^{z_+} d\bar{y}_l \\ \times e^{-\epsilon|\bar{y}_l|-\epsilon|y_l|}\,\Phi(y_l,\bar{y}_l)\,.\end{aligned} \tag{C7}$$

The $\bar{y}_l$-integration of this expression can be done explicitly and results in $\mathcal{Z}_{\rm comb}=0$. This proves our claim that the sum of all $O(N)$ contributions which have N contact terms on one side of the cut, vanishes.

APPENDIX D: DERIVATION OF THE RADIATION CROSS SECTION (4.15)

The radiation cross section (4.15) is obtained by inserting the path-integral M of (4.13) and the function F of (4.11) into (4.11). To simplify the path-integral M, we change coordinates

$$\mathbf{r}_a(\xi) = x\,\mathbf{r}_3(\xi) + (1-x)\,\mathbf{r}_2(\xi)\,, \tag{D1}$$
$$\mathbf{r}_b(\xi) = \mathbf{r}_3(\xi) - \mathbf{r}_2(\xi)\,, \tag{D2}$$

and we introduce relative and average pair coordinates

$$\hat{\boldsymbol{\rho}}(\xi) = \mathbf{r}_a(\xi) - \mathbf{r}_1(\xi)\,, \tag{D3}$$
$$\bar{\boldsymbol{\rho}}(\xi) = \mathbf{r}_a(\xi) + \mathbf{r}_1(\xi)\,. \tag{D4}$$

In terms of these coordinates, the path-integral M of (4.13) reads

$$\begin{aligned}M(\mathbf{r}_1,\mathbf{r}_2,\mathbf{r}_3|y_l,\bar{y}_l) = \int \mathcal{D}\hat{\boldsymbol{\rho}}\,\mathcal{D}\bar{\boldsymbol{\rho}}\,\mathcal{D}\mathbf{r}_b \\ \times\exp\left[i\frac{E}{2}\int_{y_l}^{\bar{y}_l} d\xi\left(\dot{\hat{\boldsymbol{\rho}}}\cdot\dot{\bar{\boldsymbol{\rho}}}+(1-x)\,x\,\dot{\mathbf{r}}_b^2\right)\right] \\ \times\exp\left[-\frac{1}{2}\int_{y_l}^{\bar{y}_l} d\xi n(\xi)\sigma\left(\hat{\boldsymbol{\rho}}+(1-x)\,\mathbf{r}_b\right)\right]\,.\end{aligned} \tag{D5}$$

The path-integral over $\mathcal{D}\bar{\boldsymbol{\rho}}$ can be done analytically (see Appendix B of Ref. [12] for more details on this step)

$$\begin{aligned}M(\mathbf{r}_1,\mathbf{r}_2,\mathbf{r}_3|y_l,\bar{y}_l) = -\left(\frac{E}{2\pi\,i(\bar{y}_l-y_l)}\right)^2 \\ \times e^{\frac{iE}{2(\bar{y}_l-y_l)}\left[2\bar{\mathbf{y}}\cdot(\mathbf{v}+\mathbf{s})+\mathbf{v}^2-\mathbf{s}^2\right]} \\ \times\int\mathcal{D}\mathbf{r}_b\exp\left[\int_{y_l}^{\bar{y}_l} d\xi\left(i\frac{E\,(1-x)\,x}{2}\dot{\mathbf{r}}_b^2\right.\right. \\ \left.\left.-\frac{1}{2}n(\xi)\sigma\left(\hat{\boldsymbol{\rho}}_{\boldsymbol{s}}+(1-x)\,\mathbf{r}_b\right)\right)\right]\,,\end{aligned} \tag{D6}$$

where

$$\mathbf{v} = x(\mathbf{u}-\bar{\mathbf{y}}) - x\mathbf{r}_3(y_l) - (1-x)\mathbf{y}\,, \tag{D7}$$

and $\hat{\boldsymbol{\rho}}_s$ denotes the straight line path

$$\hat{\boldsymbol{\rho}}_s(\xi) = x(\mathbf{u}-\bar{\mathbf{y}}) - (\mathbf{v}+\mathbf{s})\frac{\bar{y}_l-\xi}{\bar{y}_l-y_l}\,. \tag{D8}$$

Here, we have kept the dependence on $\mathbf{r}_3(y_l)$ explicitly, since we need the corresponding derivative in (4.1). We now shift the intergration variable $\mathbf{u} \to \mathbf{u}+\bar{\mathbf{y}}$ in (4.1), replacing the partial derivative w.r.t. $\bar{\mathbf{y}}$ by the partial derivative w.r.t. $\mathbf{u}$ and doing a partial integration:

$$\sum_{m,\,n} C_A^{n+m} \quad \underbrace{\cdots}_{n} \; \overbrace{\cdots}^{m} \; \underbrace{\cdots}_{n}$$

$$= \frac{1}{A_\perp}\int_Y \int d\mathbf{y}\, d\bar{\mathbf{y}}\, d\mathbf{s}\, d\mathbf{u}\, F(\mathbf{u})\,\frac{\partial}{\partial \mathbf{u}}\cdot \times \frac{\partial}{\partial \mathbf{r}_3(y_l)} M^{(\mathbf{u}\to\mathbf{u}+\bar{\mathbf{y}})}(\mathbf{r}_1,\mathbf{r}_2,\mathbf{r}_3|y_l,\bar{y}_l)\,. \tag{D9}$$

Here, the superscript $M^{(\mathbf{u}\to\mathbf{u}+\bar{\mathbf{y}})}$ on M indicates that the $\mathbf{u}$ variable is shifted. Starting from (D6), the $\bar{\mathbf{y}}$- and $\mathbf{s}$-integration is now trivial:

$$\int d\bar{\mathbf{y}}\, d\mathbf{s}\, M^{(\mathbf{u}\to\mathbf{u}+\bar{\mathbf{y}})}(\mathbf{r}_1,\mathbf{r}_2,\mathbf{r}_3|y_l,\bar{y}_l) = \int \mathcal{D}\mathbf{r}_b \exp\left[\int_{y_l}^{\bar{y}_l} d\xi \left(i\frac{E\,(1-x)\,x}{2}\dot{\mathbf{r}}_b^2 - \frac{1}{2}n(\xi)\sigma\left(x\mathbf{u}+(1-x)\,\mathbf{r}_b\right)\right)\right]. \tag{D10}$$

The approximations used to derive (4.1) are valid to leading order $O(x)$. To this order, the path-integral in (D10) coincides with the path-integral $\mathcal{K}$ given in (4.14). To obtain our final result (4.15) for the radiation cross section, we note that the boundary condition on this path-integral is $\mathbf{r}_b(y_l) = \mathbf{r}_3(y_l) - \mathbf{y} = 0$ and $\mathbf{r}_b(\bar{y}_l) = \mathbf{u}$. We can thus replace in (D9) $\frac{\partial}{\partial \mathbf{r}_3(y_l)} \to \frac{\partial}{\partial \mathbf{r}_b(y_l)}$. The integrand of (D9) is then $\mathbf{y}$-independent, and the $\mathbf{y}$-integral cancels against the total transverse area $A_\perp$. This leads to the result (4.15).

APPENDIX E: GLUON RADIATION UP TO THIRD ORDER IN OPACITY

Here, we give explicit results for the low opacity expansion of the gluon radiation cross sections (4.15) and (6.1) up to third order. We have assumed a medium of homogeneous density n_0 and finite thickness L. By explicit calculation, we have found for $N \le 3$ that the N-th order terms are of the form (6.4). We denote by Q_j the transverse energy of the gluon after j momentum transfers from the medium, see (3.39) for definition. The $\mathcal{Z}$-factors entering (6.4) are:

Results for $\frac{d^3\sigma^{(in)}(N)}{d(\ln x)\,d\mathbf{k}_\perp}$

A. For $N=1$:

$$Z_{1,1}^{(in)} = \frac{L\,n_0}{2\,Q_1^2}\,, \tag{E1}$$

$$Z_{1,2}^{(in)} = -\frac{L\,n_0}{Q\,Q_1}\,. \tag{E2}$$

B. For $N=2$:

$$Z_{2,1}^{(in)} = n_0^2\,\frac{L^2}{4\,Q_2^2}\,, \tag{E3}$$

$$Z_{2,2}^{(in)} = n_0^2\,\frac{2-2\cos(LQ_1)-L^2Q_1^2}{2\,Q_1^3\,Q_2}\,, \tag{E4}$$

$$Z_{2,3}^{(in)} = n_0^2\,\frac{-1+\cos(LQ_1)}{Q\,Q_1^2\,Q_2}\,. \tag{E5}$$

C. For $N=3$:

$$Z_{3,1}^{(in)} = n_0^3\,\frac{L^3}{12\,Q_3^2}\,, \tag{E6}$$

$$Z_{3,2}^{(in)} = -n_0^3\,\frac{6\sin(LQ_2)-6LQ_2+L^3Q_2^3}{6\,Q_2^4\,Q_3}\,, \tag{E7}$$

$$Z_{3,3}^{(in)} = n_0^3\,\frac{Q_1^3\,[\sin(LQ_2)-LQ_2]}{Q_1^3\,(Q_1-Q_2)\,Q_2^3\,Q_3} - n_0^3\,\frac{Q_2^3\,[\sin(LQ_1)-LQ_1]}{Q_1^3\,(Q_1-Q_2)\,Q_2^3\,Q_3}\,, \tag{E8}$$

$$Z_{3,4}^{(in)} = n_0^3\,\frac{Q_1^2\,[LQ_2-\sin(LQ_2)]}{Q\,Q_1^2\,(Q_1-Q_2)\,Q_2^2\,Q_3} - n_0^3\,\frac{Q_2^2\,[LQ_1-\sin(LQ_1)]}{Q\,Q_1^2\,(Q_1-Q_2)\,Q_2^2\,Q_3}\,. \tag{E9}$$

Results for $\frac{d^3\sigma^{(nas)}(N)}{d(\ln x)\,d\mathbf{k}_\perp}$

A. For $N=1$:

$$Z_{1,1}^{(nas)} = n_0\,\frac{LQ_1-\sin(LQ_1)}{Q_1^3}\,, \tag{E10}$$

$$Z_{1,2}^{(nas)} = -n_0\,\frac{LQ_1-\sin(LQ_1)}{Q\,Q_1^2}\,. \tag{E11}$$

B. For $N=2$:

$$Z_{2,1}^{(nas)} = n_0^2\,\frac{2\cos(LQ_2)-2+L^2Q_2^2}{2\,Q_2^4}\,, \tag{E12}$$

$$Z_{2,2}^{(nas)} = n_0^2\,\frac{Q_1^3\left[2-2\cos(LQ_2)-L^2Q_2^2\right]}{2\,Q_1^3\,(Q_1-Q_2)\,Q_2^3} - n_0^3\,\frac{Q_1^3\left[2-2\cos(LQ_1)-L^2Q_1^2\right]}{2\,Q_1^3\,(Q_1-Q_2)\,Q_2^3}\,, \tag{E13}$$

$$Z_{2,3}^{(nas)} = n_0^2\,\frac{Q_1^2\,[-1+\cos(LQ_2)]}{Q\,Q_1^2\,(Q_1-Q_2)\,Q_2^2} - n_0^3\,\frac{Q_2^2\,[-1+\cos(LQ_1)]}{Q\,Q_1^2\,(Q_1-Q_2)\,Q_2^2}\,. \tag{E14}$$

C. For $N=3$:

$$Z_{3,1}^{(nas)} = n_0^3 \, \frac{6\sin(LQ_3) - 6LQ_3 + L^3Q_3^3}{6\,Q_3^5}\,, \tag{E15}$$

$$Z_{3,2}^{(nas)} = n_0^3 \, \frac{Q_3^4\left[6\sin(LQ_2) - 6LQ_2 + L^3Q_2^3\right]}{6\,Q_2^4\,(Q_2-Q_3)\,Q_3^4} - n_0^3 \, \frac{Q_2^4\left[6\sin(LQ_3) - 6LQ_3 + L^3Q_3^3\right]}{6\,Q_2^4\,(Q_2-Q_3)\,Q_3^4} \tag{E16}$$

$$\begin{aligned} Z_{3,3}^{(nas)} = {} & \frac{n_0^3\,\sin(LQ_1)}{Q_1^3\,(Q_1-Q_2)\,(Q_1-Q_3)} \\ & + \frac{n_0^3\,\sin(LQ_2)}{Q_2^3\,(Q_2-Q_1)\,(Q_2-Q_3)} \\ & + \frac{n_0^3\,\sin(LQ_3)}{Q_3^3\,(Q_3-Q_1)\,(Q_3-Q_2)} \\ & - L\frac{Q_2Q_3+Q_1Q_2+Q_1Q_3}{Q_1^2\,Q_2^2\,Q_3^2}\,, \end{aligned} \tag{E17}$$

$$\begin{aligned} Z_{3,4}^{(nas)} = {} & -\frac{n_0^3\,\sin(LQ_1)}{Q\,Q_1^2\,(Q_1-Q_2)\,(Q_1-Q_3)} \\ & - \frac{n_0^3\,\sin(LQ_2)}{Q_2^2\,(Q_2-Q_1)\,(Q_2-Q_3)\,Q} \\ & - \frac{n_0^3\,\sin(LQ_3)}{Q_3^2\,(Q_3-Q_1)\,(Q_3-Q_2)\,Q} \\ & + L\frac{n_0^3}{Q\,Q_1\,Q_2\,Q_3}\,, \end{aligned} \tag{E18}$$

[1] M. Gyulassy and X.-N. Wang, Nucl. Phys. **B420** (1994) 583.
[2] X.-N. Wang, M. Gyulassy and M. Plümer, Phys. Rev. **D51** (1995) 3436.
[3] X.-N. Wang and M. Gyulassy, Phys. Rev. **D44** (1991) 3501.
[4] M. Gyulassy and P. Levai, Phys. Lett. **B442** (1998) 1.
[5] B.G. Zakharov, JETP Letters **63** (1996) 952, **65** (1997) 615.
[6] R. Baier, Y.L. Dokshitzer, A.H. Mueller, S. Peigné and D. Schiff, Nucl. Phys. **B483** (1997) 291.
[7] R. Baier, Y.L. Dokshitzer, A.H. Mueller, S. Peigné and D. Schiff, Nucl. Phys. **B484** (1997) 265.
[8] B.G. Zakharov, Phys. Atom. Nucl. **61** (1998) 838 [Yad. Fiz. **61** (1998) 924], hep-ph/9807540.
[9] R. Baier, Y.L. Dokshitzer, A.H. Mueller and D. Schiff, Phys. Rev. **C58** (1998) 1706.
[10] R. Baier, Y.L. Dokshitzer, A.H. Mueller and D. Schiff, Nucl. Phys. **B531** (1998) 403.
[11] B.Z. Kopeliovich, A. Schäfer and A.V. Tarasov, Phys. Rev. **C59** (1999) 1609.
[12] U.A. Wiedemann and M. Gyulassy, Nucl. Phys. **B560** (1999) 345-382.
[13] B.G. Zakharov, JETP Lett. **70** (1999) 176.
[14] R. Baier, Y.L. Dokshitzer, A.H. Mueller and D. Schiff, Phys. Rev. **C60** (1999) 064902.
[15] B.Z. Kopeliovich, A. Schäfer and A.V. Tarasov, Phys. Rev. **D62** (2000) 054022.
[16] R. Baier, D. Schiff, and B.G. Zakharov, hep-ph/0002198, submitted to Ann. Rev. Nucl. Part. Sci.
[17] M. Gyulassy, P. Levai and I. Vitev, Nucl. Phys. **B571** (2000) 197.
[18] I.P. Lokhtin and A.M. Snigirev, Phys. Lett. **B440** (1998) 163. and hep-ph/0004176.
[19] U.A. Wiedemann, Nucl. Phys. **B582** (2000) 409.
[20] S.J. Brodsky and P. Hoyer, Phys. Lett. **B 298** (1993) 165.
[21] N.N. Nikolaev and B.G. Zakharov, Z. Phys. **C49** (1991) 607.
[22] J.F. Gunion and G. Bertsch, Phys. Rev. **D 25** (1982) 746.
[23] M. Gyulassy, P. Levai and I. Vitev, nucl-th/0005032 and nucl-th/0006010.